

RADIO ALTIMETER TOLERANCE OF WIRELESS AVIONICS  
INTRA-COMMUNICATIONS SYSTEMS

A Thesis

by

JOSHUA THOMAS RUFF

Submitted to the Office of Graduate and Professional Studies of  
Texas A&M University  
in partial fulfillment of the requirements for the degree of  
MASTER OF SCIENCE

Chair of Committee,	Gregory H. Huff
Co-Chair of Committee,	Jean-Francois Chamberland
Committee Members,	Robert D. Nevels
	Darren Hartl
Head of Department,	Miroslav M. Begovic

May 2019

Major Subject: Electrical Engineering

Copyright 2019 Joshua Thomas Ruff

## ABSTRACT

Avionics in modern aircraft have multiple redundant wiring paths in case of failure. The aerospace industry acquired spectrum for wireless avionics which would reduce the amount of necessary wiring, but must prove compatibility with the radio altimeters incumbent to the band for certification. This work covers the development of a reference test bed validated by radio altimeter and aircraft manufacturers. This test bed was automated in a modular framework which allowed the rapid modification of software to suit a wide variety of test conditions. This work also covers the three altimeter testing regimens which used this test bed, and the development of reporting formats which supported the creation of international standards based on these results.

## ACKNOWLEDGMENTS

I would like to thank my advisor, Dr. Huff, for giving me the opportunity to work in his lab throughout undergraduate and graduate school. Under his mentorship, my interest in electromagnetics developed into a passion which has driven my career. I would also like to thank Dr. Chamberland, who provided advice and professional guidance as I navigated undergraduate research and graduate school. Additionally, I would like to thank Dr. Fred Fisher and Dr. Dave Redman for their support over the years, especially through the transition period which followed Dr. Huff's move. Without them I could not have graduated when I did. Finally, I would like to thank my parents for their constant love and support while I attended graduate school.

## CONTRIBUTORS AND FUNDING SOURCES

This work was sponsored by the Aerospace Vehicles Systems Institute (AVSI) through Authorizations for Expenditure 76s1 and 76s2 (AFE 76s1/76s2). Project members contributed funding, equipment, and expertise without which the project would not have been completed. Project members included Airbus, Boeing, Embraer, FAA, Garmin\*, Honeywell Aerospace\*, the International Air Transport Association (IATA), Lufthansa Technik, NASA, Rockwell Collins\*, Thales\*, United Technologies Corporation, and Zodiac Inflight Innovations. The project members marked with an asterisk contributed the commercial radio altimeters tested in this work.

Thomas Meyerhoff from Airbus contributed the worst case landing scenario analysis covered in Section 2.5.2.1, and the summary of initial testing results shown in Figure 3.3. Dr. Chadi Geha provided the concept for the modified altimeter test setup shown in Figure 2.2. All other work presented in this thesis was conducted by the author.

# TABLE OF CONTENTS

	Page
ABSTRACT .....	ii
ACKNOWLEDGMENTS .....	iii
CONTRIBUTORS AND FUNDING SOURCES .....	iv
TABLE OF CONTENTS .....	v
LIST OF FIGURES .....	viii
LIST OF TABLES.....	x
1. INTRODUCTION.....	1
1.1 Motivation .....	1
1.2 History .....	1
1.3 Project Goals .....	2
1.4 WAIC Feasibility Study.....	2
1.4.1 Certification.....	3
1.4.2 The Search for a Suitable WAIC Band .....	3
1.4.3 Candidate Bands.....	5
1.4.4 Channel Modeling and Security .....	5
1.4.5 Summary and Conclusions.....	6
1.5 Selecting a Suitable WAIC Band .....	7
1.5.1 Assessment of Bands between 960 MHz and 15.7 GHz.....	8
1.5.2 Relevant WRC-15 Allocations.....	8
1.6 Overview of Radio Altimeter Functionality .....	9
1.6.1 Basic Overview and Applications .....	9
1.6.2 Calculating the Height From a Time Delay .....	9
1.6.3 Altimeter Signal Processing .....	10
1.6.4 Radio Altimeter Antennas .....	11
1.6.5 Attenuation of the Altimeter Signal in Free Space.....	12
1.6.6 Conclusions .....	12
2. METHODS .....	13
2.1 Basic Altimeter Test Bed Setup .....	13
2.2 Modified Altimeter Test Setup .....	14
2.2.1 Reading the Altimeter Output.....	14

2.2.2	Implementing the Altitude Simulator.....	15
2.2.2.1	Time Delay .....	15
2.2.2.2	Achieving Standard Loop Losses.....	16
2.2.3	Generating Interference Signals .....	17
2.2.3.1	MSK Waveform .....	17
2.2.3.2	OFDM Waveform .....	19
2.2.3.3	Dual Waveforms.....	20
2.3	Python Test Software .....	21
2.3.1	Test Main Loop .....	21
2.3.1.1	Nominal Height vs Correct Height .....	23
2.3.1.2	Sequence Control.....	23
2.3.1.3	Precision of Timing Commands .....	24
2.3.2	VSG Class .....	28
2.3.3	SCPI Class .....	29
2.3.4	Post-Processing .....	30
2.3.4.1	Parsing The Copilot Log .....	30
2.3.4.2	Mapping Interference Signals to Copilot Data.....	30
2.4	Initial ‘Waic Only’ Test Plan .....	31
2.4.1	Motivations .....	31
2.4.2	Complete Diagram .....	32
2.4.3	Breaking Point Definition .....	33
2.4.4	Test Definition .....	34
2.5	Expanding the Test Setup.....	35
2.5.1	Adding The Second VSG .....	35
2.5.1.1	Providing Isolation to the VSGs .....	36
2.5.1.2	Achieving Higher Power Interference .....	37
2.5.2	Simulating Altimeter Interference .....	38
2.5.2.1	Determining the Worst-Case Scenario Geometry.....	39
2.5.2.2	Simulating Individual Altimeter Signals .....	41
2.5.2.3	Connecting the VCO Signals .....	42
2.5.2.4	Calibrating the VCOs .....	43
2.5.2.5	VCO Protection Circuit .....	45
2.5.3	Testing Lower Altitudes.....	47
2.6	Expanded Setup Test Plans .....	48
2.6.1	Full Setup Diagram.....	48
2.6.2	Breaking Point Definition .....	49
2.6.3	In Band Testing .....	49
2.6.4	Out of Band Testing .....	50
3.	RESULTS.....	52
3.1	General Plotting Scripts.....	52
3.1.1	Height Plots .....	52
3.1.2	Stat Plots .....	54
3.2	Initial ‘WAIC Only’ Testing Regimen .....	55

3.3	Expanded In Band Tests .....	58
3.4	Out of Band Testing .....	59
4.	CONCLUSION .....	61
	REFERENCES .....	62
	APPENDIX A. FULL RESULTS FOR IN BAND TESTING .....	64

## LIST OF FIGURES

FIGURE	Page
1.1 FMCW Waveform.....	10
1.2 Basic Diagram of Homodyne Receiver Used in Radio Altimeters.....	11
2.1 Diagram of Basic Altimeter Test Setup Diagram specified in DO-155.....	13
2.2 Modified altimeter Test Setup with VSG Interference.....	15
2.3 Internal Diagram of Altitude Simulator Using Optical Delay Line.....	16
2.4 MSK Waveform at 4.3 GHz Pictured on a Spectrum Analyzer.....	18
2.5 40 MHz OFDM Waveform Centered at 4.3 GHz Pictured on a Spectrum Analyzer...	19
2.6 SCPI Class Hierarchy Diagram.....	22
2.7 Height Plot Showing Sync Error .....	27
2.8 Full Test Bench Diagram for Initial Tests.....	33
2.9 Expanded Test Bench For Wideband and Altimeter Interference.....	36
2.10 Circulator with Matched Load Added to Protect VSGs.....	37
2.11 Modifications for Higher Interference Power.....	38
2.12 Geometry Provided by Project Member Airbus for Landing Scenario.....	39
2.13 Plot of IPL Values for 15 Closest Aircraft .....	41
2.14 Diagram of Combined 16 Simulated Altimeter Signals.....	42
2.15 Double Clipper Protective Circuit.....	45
2.16 Clipped Sin Wave.....	46
2.17 Left: 40ft Altitude Simulator; Right: 95 ft Altitude Simulator.....	47
2.18 Full Test Setup Combining Various Modifications to Figure 2.8.....	49
3.1 Example Height Plot from Initial Testing Regimen.....	53

3.2	Example Stat Plot.....	55
3.3	Summary of Initial Testing Results .....	56
3.4	Comparison of Impact of Different Bandwidths of Simulated WAIC Signals on Altimeter Performance. ....	57
3.5	Results from RA Type 4 with 200MHz In Band Tests. ....	58
3.6	Preliminary Interference Mask.....	59
A.1	Performance of RA Type 1 with 200MHz In Band Tests .....	64
A.2	Performance of RA Type 2 with 200MHz In Band Tests .....	65
A.3	Performance of RA Type 3 with 200MHz In Band Tests .....	65
A.4	Performance of RA Type 4 with 200MHz In Band Tests .....	66
A.5	Performance of RA Type 5 with 200MHz In Band Tests .....	66

## LIST OF TABLES

TABLE	Page
1.1 Major Candidate Bands Researched by AFE 56 and Rated According to Suitability..	5
2.1 DO-155 Loop Losses with 60 degree Beamwidth and Worst-Case Scattering. ....	17
2.2 Example Interference Signal Table. ....	24
2.3 Example VSG State Table. ....	25
2.4 Example Copilot Export. ....	31
2.5 Example Full Dataset Table. ....	31
2.6 Test Definition For Initial Testing Regimen. ....	34
2.7 VCO Attenuation Configurations for 200ft Worst Case. ....	43
2.8 VCO Calibration Results and Corresponding Function Generator Settings. ....	44
2.9 Example Interference Signals for Wideband Testing. ....	50
2.10 Example Interference Signals For Out Of Band Testing. ....	50
3.1 Interference Power Level Above Which Reported Altitude is Impacted [?]. ....	59

# 1. INTRODUCTION

## 1.1 Motivation

Wireless digital communication systems have become ubiquitous in the public life over the past two decades. These systems have matured into a proven and reliable technology, and the aerospace industry has developed a significant interest in deploying these systems into electronics on airplanes, known as avionics. Specifically, these companies are interested in radio communication between devices on a single aircraft related to the regularity and safety of flight, rather than communications outside an aircraft or for passenger entertainment [1].

Avionics manufacturers are interested in the development, sale and deployment of sensors and devices in areas on a plane that were difficult or impossible to reach with wireless systems. Examples might include placing sensors to monitor a landing gear or internal to an engine, where rotating parts make monitoring difficult [1]. Airframers, Aircraft OEMs, and Airlines all have a vested interest in any development which could reduce the amount of copper wiring on planes, thus reducing weight and fuel costs [2]. Regulators are interested in wireless avionics systems from a safety perspective. Critical avionics systems have redundant paths wired in in case of failure, and some or all of these redundancies may eventually be replaced with wireless ones [2] [1]. This type of dissimilar redundancy is always appealing from a safety perspective. The classic example of an engine fire which destroys the physical connection to a controller (and so can't be shut off) demonstrates the utility of a wireless backup [1].

## 1.2 History

The wide array of advantages to this technology motivated various companies throughout the aerospace industry to sponsor a series of working groups to implement wireless communications systems on aircraft. The systems used in this class of applications were alternatively called Wireless Sensing Networks (WSN's) in early literature, and Wireless Avionics Intra-Communications (WAIC) systems later on. WAIC related projects were sponsored and conducted through the

Aerospace Vehicle Systems Institute (AVSI), which also directed this project. AVSI projects are funded through independent grants known as Authorizations For Expenditure (AFEs).

Three AVSI projects directly relate to WAIC: AFE 56, AFE 73, and AFE 76. AFE 56 studied the feasibility of potential WAIC systems and investigated the suitability of various bands to WAIC applications. AFE 73 took the analysis done by AFE 56 and used the work to advocate to regulators for spectrum allocation for WAIC.

### **1.3 Project Goals**

This work was funded through AVSI and managed under AFE 76. Project members include but are not limited to Airbus, Boeing, Honeywell, NASA, Rockwell Collins, Thales, and Garmin. All members contributed funding, technical, and material support to this project. The goals of this project are to perform a band sharing study for WAIC with radio altimeters, to develop a prototype for WAIC systems, and to develop the regulatory documentation necessary for the certification of WAIC systems.

The technical challenges in this project directly result from both the technical studies and the inherently political interactions with regulators performed under its predecessors. Because of this, a brief summary of the work done by the two preceding AVSI projects will be presented here, emphasizing the portions of each most relevant to this study.

### **1.4 WAIC Feasibility Study**

The WAIC Feasibility study was conducted through AFE 56, and the results of this study were published in [3]. The report is summarized here for background with significant focus placed on the search for a suitable WAIC band.

AFE 56 had three primary goals [3]:

- “Identify, characterize and prioritize the most significant obstacles currently impeding widespread use of wireless communication in flight-critical functions.”
- “Evaluate the current aircraft RF certification process and suggest possible modifications or changes.”

- “Identify the most promising avenues to certify reliable and robust wireless intra-aircraft data transmission.”

Toward these ends, investigations were performed into the certification process, suitable spectrum bands, and security concerns related to the implementation of WAIC systems.

#### **1.4.1 Certification**

Any device on an aircraft must go through a regulatory certification process, which functions as a way for regulatory bodies to declare the aircraft airworthy [3]. Both civilian and military aircraft are subjected to various certification processes. The AFE 56 working group surveyed the various standards imposed by the DoD, FAA, and ICAO (International Civil Aviation Organization), as well as international treaties governing the aviation industry. The committee took an in-depth look at the flight clearance process in use at various agencies.

The AFE 56 working group then looked at the specific challenges brought to the forefront by wireless systems [3]. The primary concerns for potential WAIC systems involved the sharing of spectrum with other legal occupants of the band, as well as intentional and unintentional interferers. The committee determined that a certification process for WAIC systems would need to account for and provide mitigation strategies for each of these various potential interferers to pass certification. Information security would also need to be guaranteed for critical systems. These considerations drove the band selection process for WAIC.

#### **1.4.2 The Search for a Suitable WAIC Band**

Members of the project management committee held discussions with the FCC to gain insight on the regulator’s perspective on allocations for potential WAIC systems prior to beginning the search for a suitable band [3]. Firstly, FCC staff recommended AVSI pursue an international spectrum allocation before focusing on domestic rule-making. Secondly, the FCC placed significant emphasis on the importance of “picking a winner” as quickly as possible in the frequency selection process. These recommendation were made in light of experience with previous international radio projects, and drove AVSI to consider only bands already allocated to aviation interests.

Initially, the committee considered the Industrial, Scientific, and Medical, or ISM bands [3]. ISM bands are subjected to limited regulations, and were quickly eliminated from consideration for WAIC devices. A wide variety of commercial devices already occupy this band, and these devices are allowed to radiate at relatively high powers. Users are afforded no regulatory protection from harmful interference due to the high operating powers in these bands, a condition which would be unacceptable for the safety focused aerospace industry. For this reason the 915 MHz, 2.4 GHz, 5.8 GHz, 24 GHz, and 61 GHz bands were eliminated from consideration for WAIC devices.

To find a suitable alternative, the committee stepped through both the US and international tables of frequency allocations [3]. The committee rated alternatives according to two goals. The first was electromagnetic compatibility with wireless sensor applications. The second goal was that a suitable band already be allocated or have potential to be allocated in a manner compatible with WAIC desired properties.

A series of criteria were used to rate the suitability of potential alternatives [3]. A band already primarily allocated to an aeronautical service was considered beneficial from the political perspective of spectrum allocations. Benign co-primary users were considered essential. The less sensitive other occupants are to the minimal level of interference from on-aircraft wireless systems, the better. Bands which possessed common allocations across international regions were also considered beneficial, because this eased the process of getting approval for WAIC use of the band.

The committee considered isolation from ISM and unlicensed allotments critical to a WAIC allocation [3]. The relatively uncontrolled emitters in these bands constituted a significant threat to on aircraft wireless, even in adjacent bands. Additionally, terrestrial point to point systems introduced the possibility of impinging extremely high radiated power levels onto aircraft that pass through their links, which made isolation from these systems desirable. Although this risk is limited to low altitudes, the committee considered it a significant safety hazard that could be avoided with the choice of band. A final consideration for allocations was isolation from Satellite (Earth to Space) allocations. Maintaining these up-link sites required significant RF power, and therefore created a similar safety hazard to the terrestrial point to point systems.

Band	Existing Allocation at Time of AFE56	Rating
4.200 - 4.400 GHz	Exclusively to Radio Altimeters	C
4.800 - 4.940 GHz	Federal FIXED and MOBILE Services	A
5.030 - 5.091 GHz	Microwave Landing System (MLS)	C
5.091 - 5.150 GHz	MLS "Expansion Band"	B
5.150 - 5.250 GHz	Unused Radionavigation, Satellite Uplink Co-Primary	B-
5.350 - 5.460 GHz	Weather, Airborne, and Terrestrial Military Radars	C
8.750 - 8.850 GHz	Civilian Doppler and Fixed Military Radars	C
13.25 - 13.40 GHz	Civilian Doppler Radars	B
15.40 - 15.43 GHz	Aeronautical Radionavigation, Bordered by Satellite Uplink	C
15.63 - 15.70 GHz	Aeronautical Radionavigation, Bordered by Satellite Uplink	C
36.00 - 37.00 GHz	Earth Exploration and Space Research Satellites	B
66.00 - 71.00 GHz	Mostly Federal Secure Short Range Communication Links	B
76.00 - 77.50 GHz	Beginning Use for Radar Sensors for Vehicles	B

Table 1.1: Major Candidate Bands Researched by AFE 56 and Rated According to Suitability.

### 1.4.3 Candidate Bands

Next, the AFE 56 committee performed a review of major candidate bands for WAIC systems [3]. The committee provided a synopsis of relevant characteristics of each candidate band. AVSI performed this process with a goal of helping future working groups to prioritize future efforts at reserving spectrum allocation. Table 1.1 shows a list of bands researched by the committee, their allocation at the time of the project, and a letter rating showing their suitability according to the criteria detailed in Section 1.4.2.

### 1.4.4 Channel Modeling and Security

Finally, the AFE56 committee surveyed two more obstacles to a finalized WAIC implementation [3]. The committee examined channel modeling for wireless sensor networks and gave an overview of security concerns. Any implementation of WSN's on aircraft had the potential to be critical to the safety of flight. Because of this, the committee stressed the importance of developing a validated channel model for the band and air-frames in use. The channel models would allow for the incorporation of the physical propagation characteristics of the wireless signals inside an airframe into the system design. Once developed, these models would improve the reliability of

WAIC designs. Because of this, the committee provided an overview of channel modeling efforts in their report and made recommendations for an approach to channel modeling efforts that might follow a new WAIC allocation.

Lastly, the committee commissioned a follow up investigation which looked into the security concerns associated with WAIC systems. A report [4] was commissioned through the University of Minnesota, which aimed to analyze the various potential threats to wireless networks on aircraft. Several threat vectors and the mitigation strategies associated with them were considered. The solutions listed were meant to be a high level overview, with an emphasis on the demonstrating that mitigation strategies existed to show the feasibility of WAIC. However, to acquire certification, each device would have to provide a detailed overview of their specific implementation of mitigation techniques to the relevant certification authority [4].

#### **1.4.5 Summary and Conclusions**

The AFE 56 project committee performed a feasibility study for wireless sensing networks on aircraft. The committee first looked at the existing path to certification for instrumentation, and came to the conclusion that this path would work for WSN's as well, provided that the applicant for certification perform the necessary extra step of explaining to the FAA the added risks of the wireless device and how these risks were mitigated [3]. The committee then performed an in depth survey of potential bands for WSN use, summarizing the desirable characteristics possessed by any candidate band. The committee provided an in depth overview of the pros and cons of each serious candidate for WAIC allocation, a brief summary of which has been included in this report for reference. Finally, the committee looked at potential channel modeling techniques and security concerns associated with wireless systems on aircraft and outlined how these would need to be addressed for a real WAIC implementation [4].

The committee came to the conclusion that although there were numerous hurdles in the way of fully realizing WAIC systems, WAIC systems were feasible and these challenges could be overcome with industry expenditure and effort. The tasks necessary for WAIC implementation were as follows:

- Obtain an allocation of for WAIC use.
- Perform band sharing studies for WAIC and incumbent services.
- Develop industry standards for channel modeling of air-frames.
- Develop industry standards for addressing security concerns for wireless networks on aircraft.
- Work with regulators to develop a streamlined certification process for wireless sensing networks based on these standards.

With the feasibility study complete, the AVSI partners moved on to the task of acquiring spectrum for wireless networks on aircraft.

### **1.5 Selecting a Suitable WAIC Band**

The process for obtaining a spectrum allocation through the International Telecommunications Union – Radiocommunications (ITU-R) is nominally an 8-year long process. The first four involved developing frequency spectrum requirements, such as bandwidth and power required, and the justification for those parameters. These requirements are then vetted through various ITU-R subcommittees, and if successful, the process results in an agenda item at a subsequent World Radio Conference.

The following four years focus on sharing studies for the different bands under consideration. These studies must demonstrate compatibility with existing services in a band and the results must be verified by the ITU-R subcommittees. The documents produced during this process can be used to support a proposal for changes to a spectrum allocation.

AVSI followed up on the work done in AFE 56 under AFE 73, which initiated the ITU-R process by developing preliminary WAIC operating characteristics. This resulted in the World Radio Conference 2012 (WRC-12) issuing Resolution 423, which awarded WAIC an agenda item at WRC-15 [5].

### **1.5.1 Assessment of Bands between 960 MHz and 15.7 GHz**

At WRC-12, the ITU recommended in Resolution 423 that bands from 960 MHz to 15.7 GHz be considered for potential WAIC allocation [6]. AVSI eliminated bands below this range because the antenna size requirements were incompatible with WAIC implementation requirements. Bands above this range were to be considered only after all possibilities in this range were exhausted.

AVSI took all bands with existing allocations to aeronautical mobile or aeronautical radio-navigation services into consideration. Bands in this range that fit this criteria were considered in an initial assessment. The purpose of the initial assessment was to eliminate bands with undue burden of a regulatory or technical nature. Technical burdens could involve an excessive number of necessary band-sharing studies or difficulty of meeting sharing requirements, while regulatory burdens could involve co-occupants of a band outside of the aerospace industry.

After the initial assessment, the 2.7-2.9 GHz, 4.2-4.4 GHz, and 5.35-5.46 GHz bands were considered the three most promising candidates for a potential WAIC Allocation. This recommendation precipitated compatibility studies for these bands. Existing ground based radar systems in the 2.8 and 5.4 GHz bands were found to be incompatible with the requirements for WAIC implementations, which left the 4.3 GHz band as the only viable option. The results of this study were used to develop a proposal for a change in the 4.2-4.4 GHz band allocation, which was submitted at WRC-15 [6].

### **1.5.2 Relevant WRC-15 Allocations**

The 2015 World Radio Conference (WRC-15) made changes to the spectrum allocations in and around the radio altimeter (RA) band [7]. The 4.2-4.4 GHz band received an allocation for WAIC systems pending the experimental verification of compatibility. Additionally, new allocations for 5G systems in the 3.7 GHz (3600-4200 MHz) and 4.5 GHz (4400-4900 MHz) bands directly adjacent to the altimeter band would lead to experimental band-sharing studies.

## **1.6 Overview of Radio Altimeter Functionality**

The allocation of the 4.3 GHz band for WAIC necessitates an experimental study on the effects of interference on radar altimeters. This section provides background information on the functionality of radar altimeters which is relevant to the experimental design and setup.

### **1.6.1 Basic Overview and Applications**

The 4.2-4.4 GHz band was previously allocated exclusively to radio altimeters and transponder systems associated with altimetry. An altimeter functions to actively and continuously provide height measurements of an aircraft above the surface of the Earth [8]. The highest degree of accuracy is expected in the approach, landing, and climb phases of flight. This accuracy must be maintained through all types of ground reflectivity.

The height measured by an altimeter has a variety of uses in safety critical systems. The height functions as an input The Terrain Awareness Warning System, which gives the pilot a “Pull Up” warning at a predetermined unsafe altitude and descent rate. The height from altimeters also functions as input for Collision Avoidance, Weather, Navigation, and Autopilot systems. Radio Altimeters are expected to operate in these functions through the lifetime of the Aircraft they are installed on, which results in Altimeters used in excess of 30 years.

### **1.6.2 Calculating the Height From a Time Delay**

There are two primary types of altimeters in use today. The first are Frequency Modulated Carrier Wave (FMCW) Altimeters [8]. FMCW altimeters use a transmitter and receiver with separate antennas. The signal from the transmit antenna travels to the ground, is reflected, and returns to the aircraft. The return time of the signal is proportional to the height of the aircraft above the surface due to the constant propagation speed of electromagnetic waves.

The signal travel time is based on the return of a signal of the same frequency as the transmit signal [8]. One method for calculating the travel time of a signal involves taking the difference between the frequency of the return signal at the current time and the frequency of the transmit signal at the current time,  $\Delta f$ . As shown in Figure 1.1, given a constant waveform, the return time

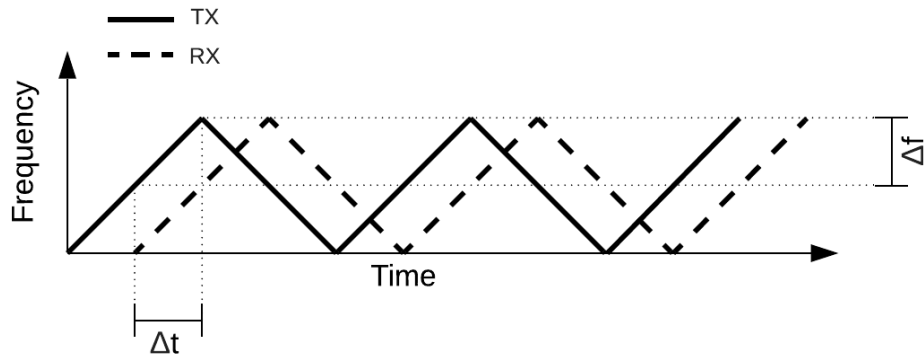


Figure 1.1: FMCW Waveform.

of a signal is:

$$\Delta t = \frac{\Delta f}{df/dt}.$$

Once  $\Delta t$  is calculated, the height can be determined using the speed of light:

$$H = \frac{c\Delta t}{2}.$$

Pulsed radar altimeters use a series of discrete pulses to track the current height of the aircraft, rather than relying on a frequency modulated waveform. The  $\Delta t$  between two pulses is used to calculate the height in the same manner that an FMCW altimeter does.

### 1.6.3 Altimeter Signal Processing

The FMCW altimeter receiver uses a homodyne detection scheme to extract data from the received waveforms. A basic diagram of this receiver is shown in Figure 1.2. At an instant in time, the waveform actively being transmitted is sampled and fed into the receiver mixer. All received signals are then down converted to baseband. Newer models apply digital signal processing to the downconverted signal. This is accomplished by applying an FFT to the received signal so that that all processing can be done in the frequency domain. Transformed data is passed to proprietary

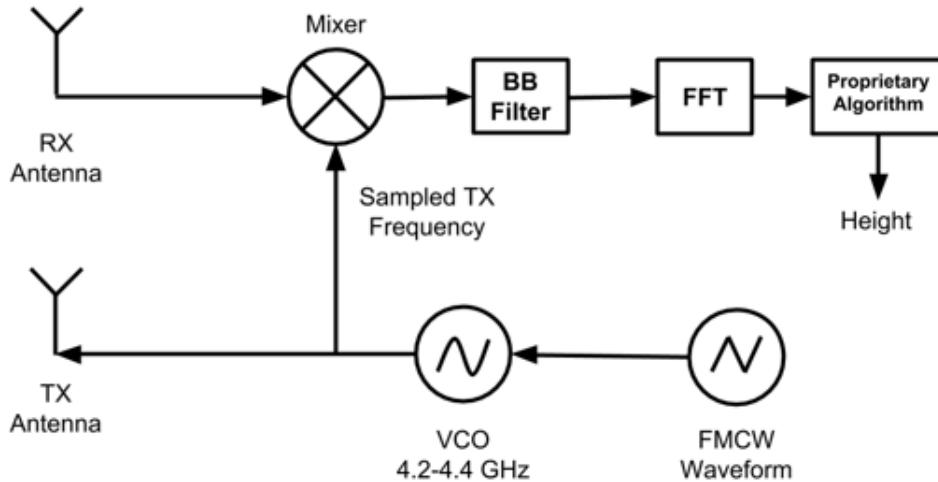


Figure 1.2: Basic Diagram of Homodyne Receiver Used in Radio Altimeters.

decision algorithms which perform an altitude estimation. Other altimeters may count the zero crossings of the received signal to determine its frequency [8]. Some units use altitude gain control and vary sweep characteristics with altitude. Pulsed altimeters use a time gating method as opposed to the frequency domain method described here for FM CW altimeters.

The varying methods of extracting the altitude data make the effects of interference unpredictable. Narrow band signals might cause occasional false readings, while signals spread across the band effectively raise the noise floor of the radar. Digital algorithms which rely on sufficient SNR to function may enter a fail state if the noise floor is raised too much resulting in “Non Computed Data-points” or NCDs [8].

#### 1.6.4 Radio Altimeter Antennas

Radio altimeter antennas require a wide half power (3 dB) beamwidth to allow the unit to function under all pitch and roll angles performed in flight. A 60 degree half-power beamwidth was chosen for these tests because it is the most commonly used beamwidth in industry. Typically patch antennas are used which results in a narrow bandwidth. The authors of [8] found no specification for cross-pol isolation for altimeter antennas in production, which eliminated a potential method of protecting altimeters from interferers. The authors also found that the necessary orientation

of an altimeter antenna toward the ground makes it vulnerable to all possible radiation sources without shielding [8] DO-155 [9] specified standard antenna beamwidths for different altimeter installations.

### 1.6.5 Attenuation of the Altimeter Signal in Free Space

A signal traveling from Altimeter transmit to ground and back to receive passes through multiple different sources of gain and attenuation. There is attenuation from cable losses, gain from the TX antenna, free space path loss as the signal travels toward the ground, loss from the scattering of the signal by the ground, path loss of the return signal, a gain from the receive antenna, and finally the attenuation from return cable losses. The combination of each of these gains and losses comprises the external loop-loss  $L$  for a signal leaving an aircraft. DO-155 operating standard [9] defines the loop loss as the ratio of the power received by the RX antenna,  $P_R$  to the power sent by the transmit antenna,  $P_T$ :

$$L = \frac{P_R}{P_T}.$$

The DO-155 standard specifies loop loss for different heights, standardized antennas, ground scattering environments, and standardized cable attenuations. The standard expands the formula shown here to incorporate these effects [9].

### 1.6.6 Conclusions

Radio Altimeters are a safety critical system in any commercial aircraft, the output of which is used by other important airborne systems. Altimeters use the time it takes a signal to travel to the ground and back to calculate the height of an aircraft off the ground, and must be able to pick up a return signal which has been attenuated significantly depending on the height. To test radio altimeters in a lab setting, both the time delay and attenuation experienced by a real signal must be simulated.

## 2. METHODS

### 2.1 Basic Altimeter Test Bed Setup

In addition to laying out performance standards for radar altimeters, the DO-155 standards [9] also specify a basic test setup for verifying an altimeter is functioning properly. Figure 2.1 shows the diagram of this test setup, which connects the RF terminals of the altimeter to an *altitude simulator* and connects a separate device to read altitude data.

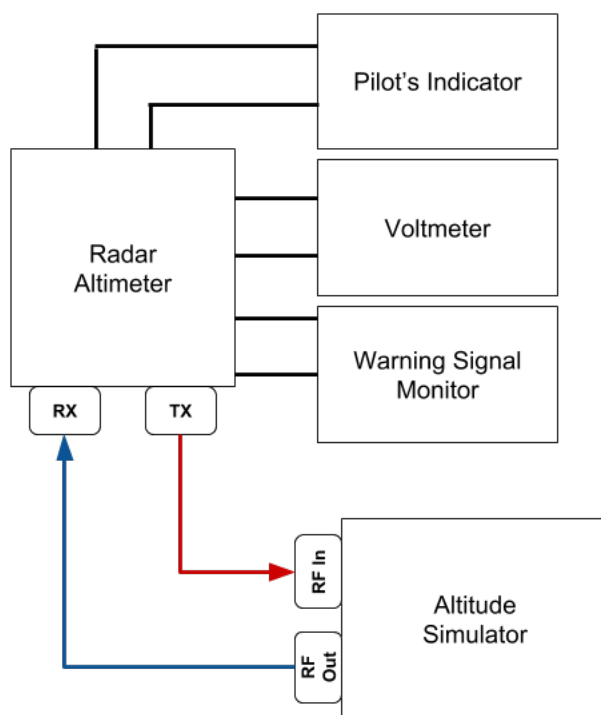


Figure 2.1: Diagram of Basic Altimeter Test Setup Diagram specified in DO-155.

The standards elaborated on the necessary characteristics of the most critical part of the test-bed, the altitude simulator. The altitude simulator needed to “consist of variable and fixed RF attenuators” [9] to simulate the loop loss an altimeter experiences aboard an aircraft (see Section 1.6.5).

The altitude simulator also needed a length of “coaxial cables or other suitable delays” [9] to simulate the physical time delay experienced by an altimeter signal between the transmitter and receiver (see Section 1.6.2). The altitude simulator directed the attenuated and delayed RF energy from the transmitter fed back into the receiver to complete the test setup.

Additionally, the standards specified that any test equipment must account for cross coupling between transmitting and receiving antennas. The setup used for these tests would be verified by radar experts to adequately compensate for that. DO-155 emphasized that the altitude simulator should achieve the desired altitude within 1% and the correct attenuation within 2.5 dB [9]. However, for the purposes of looking at the effects of interference, the absolute altitude is less important in these tests.

## **2.2 Modified Altimeter Test Setup**

AVSI designed a modified version of the altimeter test setup specified by DO-155, shown in Figure 2.2. The modifications allow the controlled injection of interference into the line after the altimeter signal passes through the altitude simulator.

### **2.2.1 Reading the Altimeter Output**

The altimeter outputs labeled height data on a standardized ARINC 429 cable configuration. The modified setup uses a Ballard ARINC device to convert the data from ARINC 429 to USB serial format, providing each data point with a time stamp. On the test laptop, Ballard CoPilot software reads the serial data and provides a display which allows the real time monitoring of all altimeter output and labels.

The labels are critical because some data points may be labeled NCD (No Computed Data) when conditions are insufficient for a reliable height measurement. CoPilot software also allows for the easy export of test data to Microsoft Excel documents for post processing.

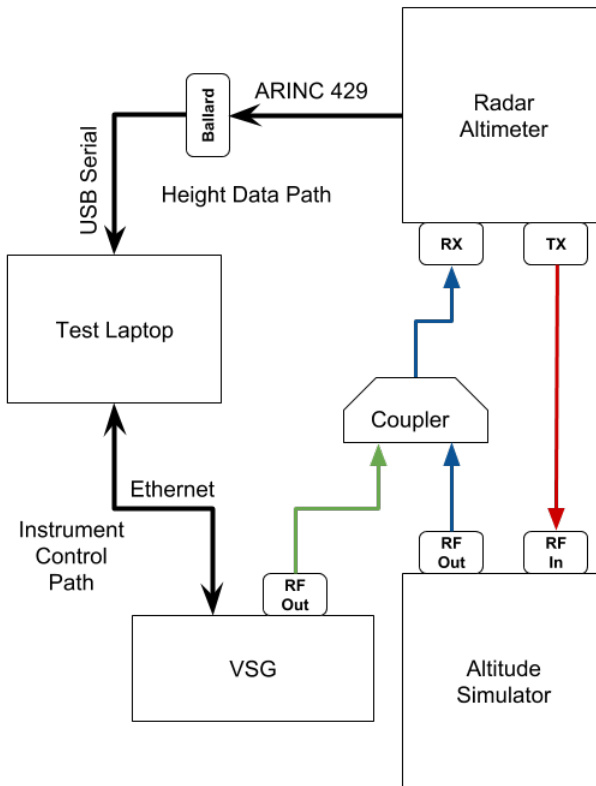


Figure 2.2: Modified altimeter Test Setup with VSG Interference.

## 2.2.2 Implementing the Altitude Simulator

### 2.2.2.1 Time Delay

Different test altitudes require the use of different methods of delaying the RF energy output by the altimeters. For the initial tests at higher altitudes, spools of fiber optic cables create a time delay as shown in Figure 2.3. The RF output from the altimeter transmitter was fed by coax connection to the fiber optic transceiver, which could either pass the signal to a single fiber optic spool or a series of cascaded spools to achieve a desired height. This setup contained optical spools of 500, 1000, 2000, and 4500 feet, each of which could be used individually or in conjunction with any or all of the other spools to implement a delay.

The optical transceiver and cascaded spools also contribute an attenuation to the loop loss

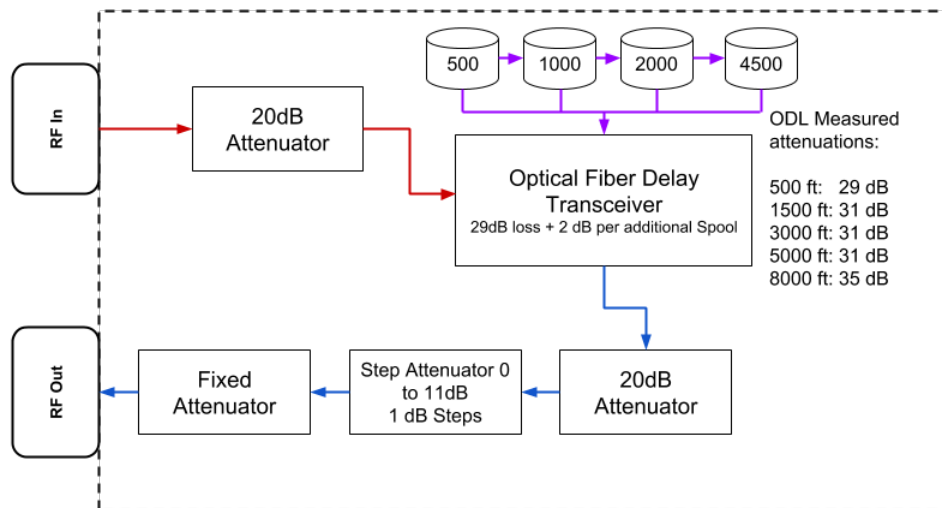


Figure 2.3: Internal Diagram of Altitude Simulator Using Optical Delay Line.

which varies based on the number of spools cascaded. A single spool setup has an attenuation verified experimentally to be 29 dB, with an additional 2 dB loss added for each additional cascaded spool.

Later tests modified this delay setup to test an altimeter in takeoff and landing scenarios. The much lower height in these scenarios made spools of coax sufficient for the delay instead of fiber optic cables. Two coax spools provided a height of 40 ft and 95 ft for testing these scenarios, with a 6 dB and 36 dB attenuation contributed to the loop loss, respectively.

#### 2.2.2.2 Achieving Standard Loop Losses

DO-155 specifies loop loss for various heights and antenna types. Table 2.1 lists the loop loss used for each height in these tests. To achieve the Loop Losses specified by DO-155 standards for each height, the attenuation inherent in the delay method used for each height must be taken into account. Once the attenuation from the delay line is subtracted from the loop loss, 10, 20 and 30 dB fixed attenuators inserted into the setup get within 10dB of the desired loop loss. The first 20 dB attenuator is located ahead of the fiber optic transceiver to protect it from damage (see

<b>Height</b>	<b>Loop Loss</b>
40ft	76 dB
95ft	84 dB
500ft	100 dB
1500ft	109 dB
3000ft	116 dB
5000ft	120 dB
8000ft	124 dB

Table 2.1: DO-155 Loop Losses with 60 degree Beamwidth and Worst-Case Scattering.

Figure 2.3. Finally, a step attenuator capable of 1 to 11 dB is used to achieve the desired loop loss with a 1 dB precision.

### 2.2.3 Generating Interference Signals

A Rhode and Schwarz SMU200A Vector Signal Generator (VSG) is used to generate simulated WAIC signals of varying modulation types, bandwidths, and power levels. The VSG has a SCPI interface which allows an external computer to control any functionality on the instrument through commands sent over either a serial or an Ethernet connection.

The AFE76 Project Management Committee (PMC) chose the modulation formats to represent candidate WAIC interference. The PMC chose to subject the altimeters to an MSK waveform, as well as OFDM waveforms of varying bandwidths and dual versions of both waveforms. These waveforms were chosen because of their similarity to systems in use for GSM and LTE cellular networks. This meant chipsets were widely available (designed for other frequencies), and WAIC networks could be modeled after purchased IP instead of developed from scratch. Each waveform used “junk” data to modulate the carrier, which consisted of randomly generated ones and zeros with equal probability of either.

#### 2.2.3.1 MSK Waveform

MSK or Minimum-Shift Keying is a type of modulation format which can be considered as a form of Phase-Shift Keying (PSK) or as a special case of Frequency Shift Keying (FSK) [10]. The

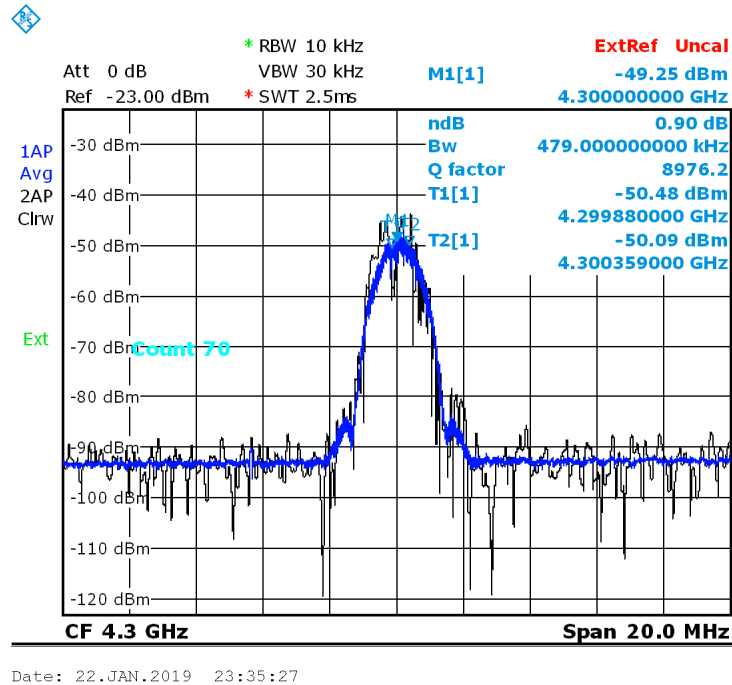


Figure 2.4: MSK Waveform at 4.3 GHz Pictured on a Spectrum Analyzer.

frequency separation of an MSK signal,  $\Delta f$  is:

$$\Delta f = \frac{1}{2T}$$

and, thus, it has a modulation index of 1/2. This is “the minimum frequency separation for orthogonality of the two sinusoids” [10]. An MSK waveform is shown on the spectrum analyzer screen-cap in Figure 2.4.

MSK modulation is available natively in the VSG software through the *custom waveform* interface. The Rhode and Schwarz VSG provides a number of common modulation options in this interface for the user to choose from. This simplifies the waveform generation for this case, as every in-built functionality on the VSG has a SCPI command corresponding to it.

### 2.2.3.2 OFDM Waveform

Orthogonal Frequency-Division Multiplexing or OFDM attempts to achieve an efficient, wide-bandwidth communication system by “dividing the channel bandwidth into equal-bandwidth sub-channels, where the bandwidth of each sub-channel is sufficiently narrow so that the frequency response [...] of sub-channels are nearly ideal” [10]. An OFDM waveform is shown on the spectrum analyzer screen-cap in Figure 2.5. One way to view the OFDM waveform is as a series of

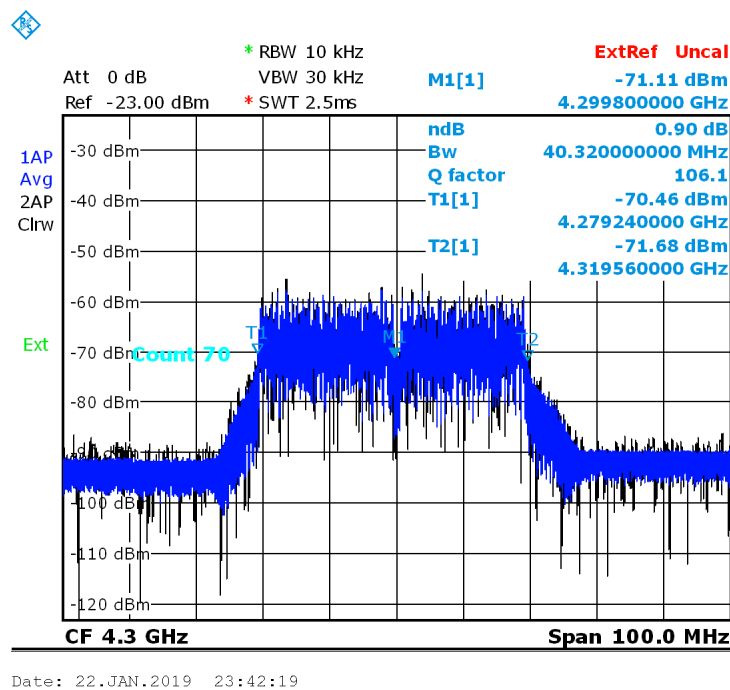


Figure 2.5: 40 MHz OFDM Waveform Centered at 4.3 GHz Pictured on a Spectrum Analyzer.

MSK waveforms spread out orthogonally along a desired bandwidth. From this perspective, MSK can be seen as the minimum bandwidth version of a system based on OFDM, and the altimeter can thus be subjected to wider and wider bandwidth systems to show the response to a greater number of WAIC devices on (or external to) an aircraft. This aspect, as well as the similarity of an OFDM signal to LTE systems, made it a very attractive option for testing the impact of WAIC.

Generating OFDM signals with the VSG was a more involved process than generating MSK, because the functionality for creating OFDM was not available natively in the VSG software. Consequently, OFDM had to be generated through the VSG's *Arbitrary Waveform Generator*. The arbitrary waveform generator enables the VSG to generate any waveform from IQ data stored in a file on the VSG. The SCPI command for generating an arbitrary waveform must include the file path for this IQ data.

This enabled an OFDM waveform to be specified by a Matlab script which exports raw IQ data, which is then converted to a form readable by the VSG through proprietary Rhode and Schwarz software. The conversion software allowed the user to adjust the clock rate, thus adjusting the bandwidth of the signal used. The bandwidth could then be measured with a spectrum analyzer to verify the process has yielded the expected waveform. The bandwidth of the OFDM waveform was defined as being 6 dB down from the peak envelope power.

### 2.2.3.3 *Dual Waveforms*

The VSG allows full control of an RF generator along with two baseband generators. The RF generator gives the user control of RF carrier frequency as well as the output power level of the carrier in dBm. The baseband generators allow the modulation of two potentially unique waveforms onto the carrier wave, with a possible offset frequency from the center. Both dual MSK waveforms and dual OFDM waveforms of bandwidth less than 40 MHz were tested using a +/-20 MHz offset between them.

Dual waveforms were considered an important option for testing due to a special characteristic of some altimeters at low altitudes. As the plane descends, the sweep rate of an altimeter increases to give more frequent readings at a more safety critical phase of flight. This is done by significantly reducing the  $\Delta f$  covered by the altimeter FMCW. The effects of this offset were thus investigated to determine whether WAIC's impact could be minimized at critical altitudes by leaving the center of the band clear.

## 2.3 Python Test Software

Python code written by the author pieces together the various parts of this setup into an integrated test bench. The goal was to coordinate ARINC 429 signals gathered independently through the Ballard device with signals generated independently using the VSG. Additionally, software needed to manage large datasets for post processing. Different Python scripts control the various functions of the test bench. These include:

- Database Creation,
- Signal Generation,
- Data Parsing,
- Time Stamp Coordination,
- Plotting and analyzing the results.

The software uses Standard Commands for Programmable Instruments or SCPI to control the vector signal generator. In this test bed, the SCPI instructions are processed through an object-oriented hierarchy shown in Figure 2.6. The super-class, SCPI interfaces directly with all lab equipment. The subclass, called *RS\_Signal\_Generator* in this implementation, contains Python functions associated with all instrument specific commands. The helper functions from SCPI send and receive communication with the instrument. Finally, the main loop exists at the highest level, which times the calls of different instrument commands and creates a database to store them. The idea behind this abstraction is to prevent the main loop from dealing with any raw SCPI command syntax – this should only be handled by one of the instrument classes.

### 2.3.1 Test Main Loop

The highest level of this design is the test main loop. The test main loop creates the SQLite database which stores all important information for easy transfer between the different Python scripts necessary for the test bed. This program also contains variables for various test parameters,

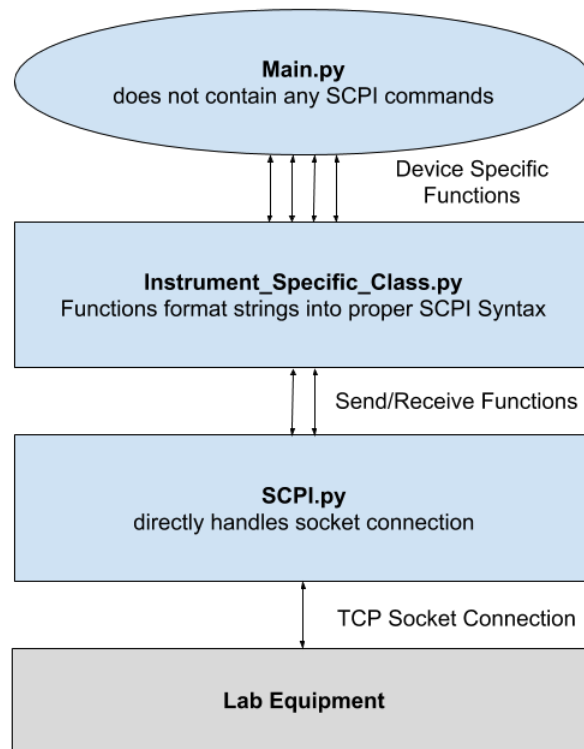


Figure 2.6: SCPI Class Hierarchy Diagram.

which are stored in an SQLite database for easy reference and sometimes directly control the sequence of a test. Finally, this program loops through the sequence interference signals specified by the various test parameters, and sends the commands to the VSG to generate them. The commands sent to the VSG are time stamped as precisely as possible, and recorded in the *Generated Signals* table in the database.

Certain test parameters are stored for reference or calculation but do not directly affect the sequence of interference signals to be generated. These include the altimeter make and model, the nominal height of the test setup, the loss experienced by interference signals traveling to the altimeter RX, and the loop loss used in the setup. Other parameters directly control the sequence of the test, including interference on and off times, power levels to be used, modulation formats to be tested, and RF carrier frequencies to be used.

### 2.3.1.1 *Nominal Height vs Correct Height*

*Nominal height* is the term used to refer to the approximate altitude determined by the experimental test setup. The difference between measured height and the nominal height of the setup varies between the different altimeters, and is primarily a result of different calibration settings for each altimeter. The calibration procedure is an important part of installing an altimeter onto an aircraft. When an aircraft is on the ground, the TX and RX antennas used by the altimeter are naturally several feet off the ground, in line with the airframe. Additionally, there are standardized delays from the altimeter TX port to the TX antenna and from the RX antenna to the RX port. These are known as Aircraft Internal Delays (AIDs). To compensate for the varying heights of airframes, as well as the AID installation, avionics manufacturers developed a calibration procedure so that each altimeter could be programmed upon installation to output an altitude of 0 ft when the plane is on the ground.

Because these tests are only concerned with a differential *height error*, rather than the accuracy of an absolute altitude measurement, *nominal height* is only used to set the loop loss. Instead, the baseline measured height with no interference, or *correct height*, is calculated in post processing as the median altitude over a several minute period when the VSG is in the OFF state before the test begins. Any height error attributable to interference is measured as a distortion from this correct height. Because of this, calibration of each altimeter to the setup is unnecessary.

### 2.3.1.2 *Sequence Control*

The primary purpose of the test main loop is to subject an altimeter to various modulation formats, gradually stepping up the power of each until the altitude readings from an altimeter are distorted or broken. The main loop determines the type of modulation, power level, and timing, and as each signal is turned on or off by the VSG, stores the parameters for the signal in the *Interference Signals* table for use in post processing, an example of which is shown in Table 2.2. Each unique modulation format and power combination will have two entries in the *Interference Signals* table, corresponding to the RF ON and RF OFF states of the VSG.

ID	Altimeter	Start Time	End Time	Modulation	Carrier Freq	Power	RF State
1	Alt A	19:23:06	19:23:07	MSK	4300 MHz	-10 dBm	OFF
2	Alt A	19:23:07	19:23:08	MSK	4300 MHz	-10 dBm	ON

Table 2.2: Example Interference Signal Table.

A variety of parameters controls the progression of different interference signals. The *interference\_duration* and *signal\_off\_duration*, define the length of time the altimeter will be subjected to a particular interference signal, as well as the length of time the altimeter will have to recover from any error caused by the previous signal. Throughout the main loop, each signal’s Start Time and End time is calculated using interference duration variables.

A range of RF powers is specified using *power\_min*, *power\_max*, and *power\_step*. For a given modulation format, the main loop iterates through each power level in this range, subjecting the altimeter to this interference power. This allows the user to step through increasing power with as much granularity as is desired for the test.

The final variable, which is important to the progression of a test, is a list called *modulation\_formats*. This list contains strings corresponding to the different modulations the VSG will generate. MSK and OFDM signals of varying bandwidths will be listed here. The main loop iterates through each string in this list, passing the string to helper functions.

The first helper function is a lookup which calls the proper function in the VSG class corresponding to a specific modulation format string. The second helper function gives the option for different modulation formats to be put on different carriers, or a list of different carrier functions. Iterating through different carriers for different modulation formats proved to be a critical functionality in later tests.

### 2.3.1.3 Precision of Timing Commands

During initial testing phase of the main loop, problems occurred which prevented the *interference\_duration* and *signal\_off\_duration* from precisely controlling the duration and recovery time of an interference signal. This section provides an overview of the different timing issues encoun-

ID	Timestamp	RF State	Power	PEP	Carrier	Offset 1	Custom 1	Arb 1
1	11:49:39.96	1	-3 dBm	4.48	4300 MHz	0	0	1
2	12:09:40.26	0	-3 dBm	4.48	4300 MHz	0	0	1

Table 2.3: Example VSG State Table.

tered over the course of these tests, as well as the approaches taken to mitigate each issue.

The first and most serious type of issue encountered while running these tests was termed *hanging delays*. These occurred when the main loop progressed more or less as expected, but the vector signal generator would “hang” in its previous state for a significant period of time after the command was sent.

To address this problem, the program was modified and a new table was added to the database to store the Vector Signal Generator state after each set of commands. Since the purpose of this table was only to be used for debugging, entries were kept as simple as possible. For example, a 1 in *RF State* corresponds to RF ON. Conversely, a 0 in *RF State* corresponds to the RF OFF setting. The *Power* and *Carrier* columns correspond with the same values in Table 2.2. *Offset 1*, *Custom 1*, and *Arb 1* correspond to the state of the first Baseband generator, telling whether the *Custom Waveform Generator* corresponding to a MSK Waveform (see Section 2.2.3.1) or the *Arbitrary Waveform Generator* (see Section 2.2.3.2) corresponding to an OFDM waveform are active, respectively.

For the purposes of the timing problem, these attributes serve as a fingerprint, allowing an investigator to correlate each row in the VSG State Table to a row in the Interference Signals table. Information here may seem redundant, but this value differs notably from the values in the interference signals table in that the VSG state table is only populated *with values received from the Vector Signal Generator*. Because of this, this table allows for a simple method for looking through the data to find at which point the VSG might “hang” in its current state rather than switch to the next signal as specified in the interference signals table.

Using this method, different theories for potential causes of the hanging delays were inves-

tigated. The first potential problem was dropped or delayed packets. During the initial setup, instruments were connected to one another over the TAMU network. This was functional but introduced latency during times of heavy network traffic. These issues were solved by moving the VSG and controller laptop onto their own local network.

The deployment on a local network addressed the most severe issues with latency, but it did not eliminate the delays entirely. Remaining delays were attributed to a slowdown in the processor handling the sequence of Python commands. These remaining delays would only occur at times of extremely heavy CPU usage (possibly caused by a memory leak in the old Ballard driver), and were eliminated almost completely by rebooting the controller laptop more frequently. Later on, an upgrade to the Ballard driver reduced these even further.

The VSG State table revealed another source of imprecision in timing commands. It was noticed that the VSG State would not change until nearly a second longer than the *Interference Duration* or *Signal off Duration* parameters specified. This drift occurred because the main loop used Python in-built `Sleep()` function to handle timing. The sleep function used the exact interference duration passed as a parameter. After the program ‘woke up’, the commands to set the next interference signal up would be called, thus introducing a small delay beyond the specified duration.

This problem was dealt with by replacing the `Sleep()` function with a custom function called `Wait_Until()`. This new function takes the signal end time as a parameter (see Table 2.2), subtracts the current time from the end time, and uses the new value as the parameter for Python’s in-built sleep function. This allows the next end time to be calculated in advance by adding the *Interference Duration* or *Signal off Duration* to the previous signal’s end time, and storing the previous signal’s end time as the start time for the next signal.

Using the *wait until* method to time commands offered important new flexibility to the main loop. This method allows writing signals to a database, setting up the baseband generators, and pinging the VSG for the VSG State information all to occur while the VSG is in an RF OFF state. Although the VSG settings cannot be adjusted in RF ON without compromising the integrity of the

signal, other tasks such as writing to the database and pinging the VSG for state information can be performed. When these are completed, the *wait until* function will still wake the program at the proper time to turn the VSG on or off. The implementation of the *wait until* function eliminated the drift problem, and allowed for the *Interference Duration* and *Signal Off Duration* parameters to precisely control the signal on and off time.

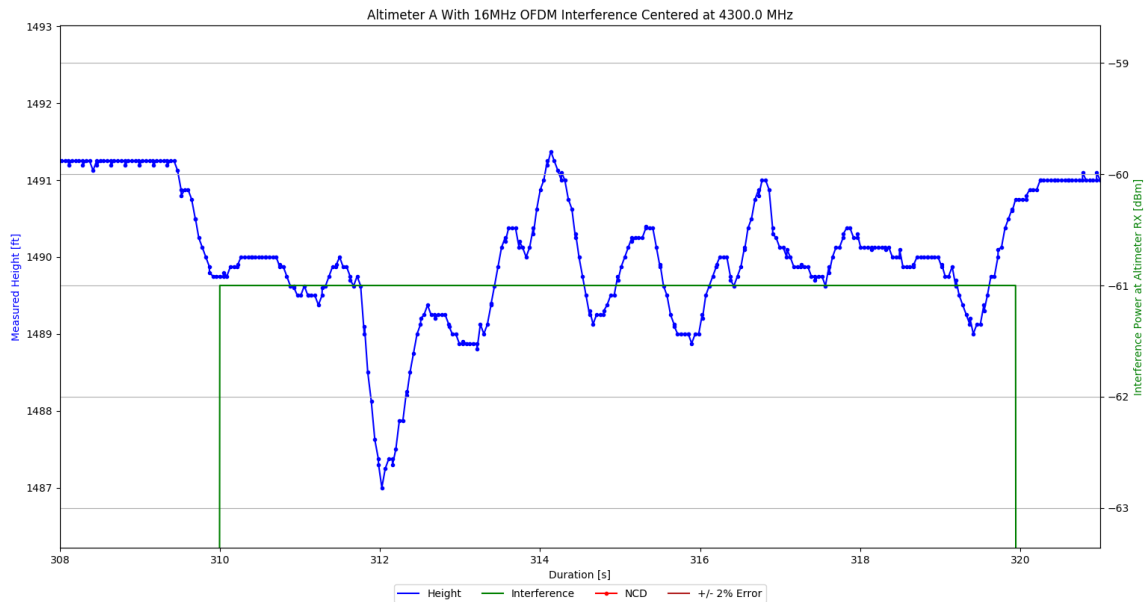


Figure 2.7: Height Plot Showing Sync Error

The final problem encountered involved the synchronization of time stamps of data between the controller laptop and the Ballard ARINC device. The Ballard internal clock drifted from about half a second ahead of the controller laptop clock to about half a second behind. This led to data sets such which looked like Figure 2.7, where distortion from the correct height would appear a split second before the interference signal was turned on. Additionally, due to averaging techniques used in the altimeter’s signal processing, there would be several data points during which the altitude would recover from the distortion caused by any interference.

This issue could not be fixed completely, although several different approaches were taken

to mitigate it. Firstly, the Ballard used in initial testing was an older unit, which meant it was more prone to clock errors. To address this, the clock was driven by an external IRIG-B timecode signal, rather than the on board IRIG [11]. A program called NMEA time generated the IRIG signal through the controller laptop's audio jack, which was then fed into the Ballard input. These changes would not completely synchronize the Ballard, but it would limit the drift of one clock away from another throughout a test.

Later on, when a new Ballard was purchased for this project, the external IRIG signal was no longer needed, as the updated Ballard driver provided adequate synchronization over USB. Another technique used to prevent any loss of synchronization was to periodically power cycle the Ballard to ensure that the clock is reset. Finally, to minimize the impact of any data points not captured in the RF ON interval by post processing, long interference durations were used to ensure that the impact of any missed points on the true average was minimized.

### 2.3.2 VSG Class

The VSG Class allows the main loop to create an object corresponding to each VSG connected to the network in the lab setup. This object then has access to functions which perform every operation needed by the main loop. The VSG Class inherits functionality from *SCPI.py* common to every SCPI programmable instrument. The VSG class provides functionality for controlling both the RF generator, as well as the VSG's two baseband generators.

The general purpose of each function in the VSG class is to construct the string for each SCPI command corresponding to that function, and send the command using the inherited SCPI *send* function. For example, the following SCPI command sets Baseband A to MSK modulation:

*“SOUR1:BB:DM:FORM MSK.”*

“SOUR1” corresponds to baseband generator A, where “SOUR2” would correspond to baseband generator B. Different SCPI commands have different parameters like this which the VSG class takes in as a normal Python variable and inserts into the string.

The VSG class provides several functions which perform this task for the RF Generator. RF

ON and RF OFF commands are self explanatory, while the *set\_carrier* function lets the user choose a carrier frequency as well as the RF power setting.

Similarly, the VSG class offers functions which will set the custom modulation format of either baseband generator (for setting MSK), or for setting the arbitrary waveform generator in each baseband generator (for setting OFDM). This class also provides functions for enabling and disabling the baseband generators, which is necessary for switching between dual and single modulation formats.

Lastly, the VSG class will have functions for setting a dual MSK or dual OFDM waveform. These will make two calls to the single MSK or OFDM function within VSG, simply passing a different source parameter to specify a different baseband generator.

### 2.3.3 SCPI Class

*SCPI.py* contains the ‘lowest’ level of programming in the SCPI hierarchy shown in Figure 2.6. The goal of this abstraction was to implement a small set of core functionality that would be needed for any instrument capable of running SCPI commands. The SCPI class handles the TCP connection, sends and receives all commands and queried data from the instrument, and contains a few other universal instrument commands.

The first task handled by SCPI is the initialization of the socket connection between the controller laptop and the instrument. The constructor takes in the IP address of the instrument and the port number, and uses the Python socket class to initialize the connection. When the experiment is over, the `SCPI.close` function which handles the proper termination of the socket connection.

Next, the SCPI class creates custom send and receive commands inherited by every instrument object. The send command handles the proper encoding of any SCPI command string before calling the native socket class `send` function. The receive command decodes a received string from the instrument, and parses the string into the different array elements delimited by commas in SCPI syntax. The receive command is meant to be called within any subclass command which queries the instrument for information, as the data types received will vary depending on the query.

Finally, there are a few other commands universal to almost every SCPI controlled device. The `reset` command ensures the instrument begins each experiment from a clean state. The `operation complete` query is called between commands to ensure that no commands are executed out of order. Last, the `identify` query returns the instrument make and model information, which is useful when first setting up an instrument for automation.

### 2.3.4 Post-Processing

After the test sequence is completed, a series of other Python scripts are used to post process the newly generated data. Time stamped altitudes must be exported from the Ballard CoPilot software into an Excel document, and a python script has to read the data from this log into the SQLite database. A second program uses the time stamps from both the logged altitude table and the generated signals table to create a full data set, where each altitude measurement is labeled with the type and magnitude of interference the altimeter was subjected to at that time. Finally, several Python scripts take this full dataset and use it to generate plots which aid in the interpreting of the results.

#### 2.3.4.1 Parsing The Copilot Log

The first post processing script parses the Ballard Copilot log into the SQLite database so that it can be used by other scripts. The CoPilot export is in an excel file formatted like Table 2.4. This table is read by python using SQLite's built in `read_excel` function. Most of the data is then added to the SQLite database as is, but the `Value` string is stripped of units and cast as a float so that the numerical value can be easily used by other scripts.

The most important columns are the `Value`, `Time`, and `Activity` label. The `Activity` label reads 'SSM ERROR' whenever the altimeter does not receive a strong enough signal to make a reliable altitude calculation. Points with this flag are called NCD or Non-Computed Data.

#### 2.3.4.2 Mapping Interference Signals to Copilot Data

The next post processing script maps each of the Altitude data points from the copilot log (Table 2.4), and maps them to the interference signal (Table 2.2) active at that time. The method for

Item #	Ch#	Lbl#	Value	Time	Activity	Name
0	0	165	509 feet	26:45.4	LO	Radio Height
1	0	165	509 feet	26:45.5	LO SSM ERROR	Radio Height

Table 2.4: Example Copilot Export.

ID	Timestamp	Ch#	Carrier	Altimeter	Height	Modulation	Power	Status	RF
0	13:54:40.5	0	4300	Alt A	506	80 MHz OFDM	7	LO	ON
1	13:54:40.6	0	4300	Alt A	506	80 MHz OFDM	9	LO	OFF

Table 2.5: Example Full Dataset Table.

mapping them is simple: if the time stamp for the data point is greater than an interference signal’s *start time* and less than the same interference signal’s *end point*, the altitude data is labeled with the corresponding modulation format, RF Power, RF State, and Altimeter under test information from the interference signals table. This process is repeated until all data points have been mapped.

## 2.4 Initial ‘Waic Only’ Test Plan

The test setup design described above gave a wide degree of flexibility to the type, magnitude, and timing of interference the altimeters could be subjected to. Preliminary tests helped to develop and debug the test setup, but were not comprehensive enough to draw conclusions from. This covers the development questions of for and the execution of the first comprehensive test regimen. Additionally, this section pieces together the components discussed earlier into a complete test diagram.

### 2.4.1 Motivations

The initial testing regimen had a series of questions about the behavior of real altimeters in the presence of interference that needed to be answered:

- At what power level will *any* MSK or OFDM signal at 4.3 GHz ‘break’ an altimeter?
- Does the ‘breaking point’ an altimeter depend on the bandwidth of the signal?

- Does adding separation between interference signals at the center influence the ‘breaking point’?
- How does the positioning of a signal within the altimeter band affect the breaking point?
- The *definition* of precisely what ‘breaking point’ means in the context of these tests also needed development.

A discussion of preliminary testing between the PMC and the author in the context of these driving motivations led to development of the methods discussed in earlier sections which culminated in the test procedure discussed here.

#### **2.4.2 Complete Diagram**

The diagram of the Modified Test Setup in Figure 2.2 gives conceptual background to the tests, and Figure 2.3 gives detailed insight into the operation and configuration of the altitude simulator. However, neither is detailed enough to provide the context necessary for a complete test description. Figure 2.8 shows the full test setup used in detail. A full page version is provided in Appendix A.

This diagram shows the altitude simulator embedded into the full test setup, as well as measured path attenuations with the step and fixed attenuation set to zero. The measured path attenuations are then used to determine a value for the fixed attenuator (10,20, or 30dB), and a value for the step attenuator (1-11dB) to precisely achieve the DO-155 specified loop loss between TX and RX. Table 2.1 shows the loop loss values used for the different heights in this setup.

For 500 ft, which had the lowest attenuation, the loop loss from TX to RX was just within the dynamic range of a network analyzer, and so could be verified experimentally with a single S21 measurement. Higher altitudes could not be verified in this manner, but because the measurement closely matched calculations for 500 ft, extrapolating to higher altitudes and loop losses was reasonable.

Several elements not shown in the conceptual diagram from Figure 2.2 are added in Figure 2.8. The output of the VSG is divided between the interference injection point and a spectrum analyzer

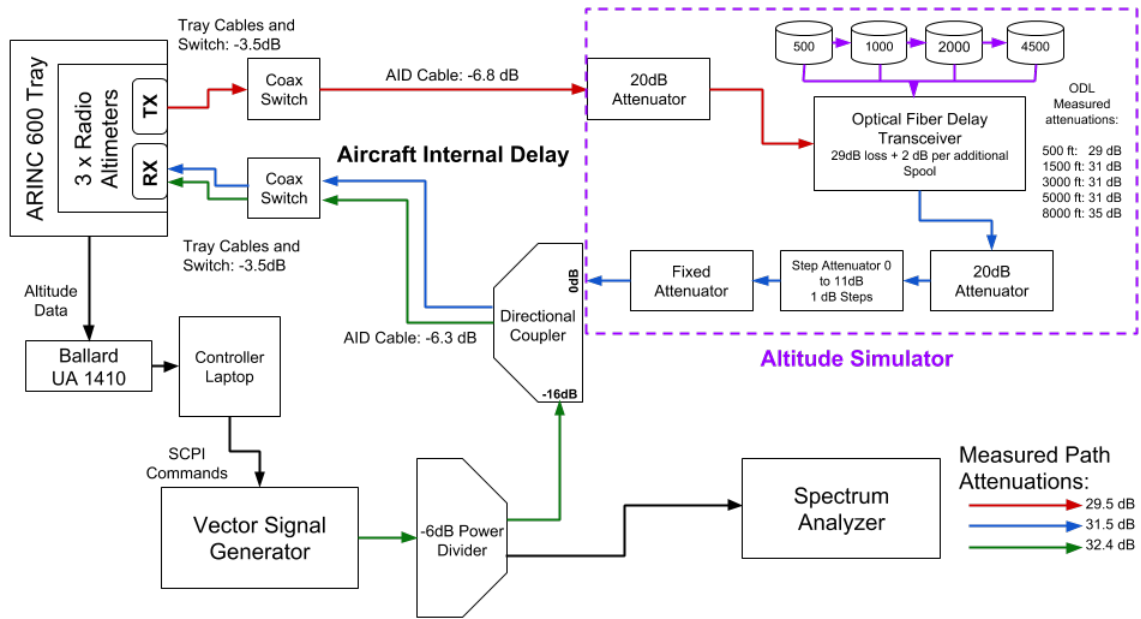


Figure 2.8: Full Test Bench Diagram for Initial Tests.

using a 6 dB resistive coupler. The spectrum analyzer allows the test operator to view the interference signals actively being tested, and make adjustments to the setup when they do not match expectations. A directional coupler allows interference to be inserted into the altimeter line at the injection point without adding additional attenuation to the loop.

Other elements pictured which weren't on the original diagram include coax switches and an ARINC 600 tray. The tray and switches are necessary in part because the DC power supply to each altimeter is different, and the tray acts as a protection from damage. Additionally, they allow for quick and easy alternating between the various altimeters under test, which is important in case any of this is ever actually flight tested.

### 2.4.3 Breaking Point Definition

The purpose of these tests was to search for an altimeter's 'breaking point' under various scenarios of interference. Performance standards for radio altimeters first set out in DO-155 were updated in the ARINC 707 standards [12]. The standards stated that "radio altimeter accuracy, when measured in accordance with RTCA DO-155, [should] be within 1.5 feet or 2%, whichever

Modulation	Interference Signal			VSG RF Power			Durations	
	Bandwidth	Center	Offset	Min	Step	Max	ON	OFF
MSK	5 MHz	4300 MHz	0 MHz	-60 dBm	2 dB	10 dBm	10 s	10 s
Dual MSK	5 MHz	4300 MHz	20 MHz	-60 dBm	2 dB	10 dBm	10 s	10 s
OFDM	5 MHz	4300 MHz	0 MHz	-60 dBm	2 dB	10 dBm	10 s	10 s
Dual OFDM	5 MHz	4300 MHz	20 MHz	-60 dBm	2 dB	10 dBm	10 s	10 s
OFDM	10 MHz	4300 MHz	0 MHz	-60 dBm	2 dB	10 dBm	10 s	10 s
Dual OFDM	10 MHz	4300 MHz	20 MHz	-60 dBm	2 dB	10 dBm	10 s	10 s
OFDM	20 MHz	4300 MHz	0 MHz	-60 dBm	2 dB	10 dBm	10 s	10 s
Dual OFDM	20 MHz	4300 MHz	20 MHz	-60 dBm	2 dB	10 dBm	10 s	10 s
OFDM	40 MHz	4300 MHz	0 MHz	-60 dBm	2 dB	10 dBm	10 s	10 s
OFDM	80 MHz	4300 MHz	0 MHz	-60 dBm	2 dB	10 dBm	10 s	10 s

Table 2.6: Test Definition For Initial Testing Regimen.

is greater.” WAIC or out of band interference needed to demonstrate that it distorted the altitude signal less than these standards. Thus, the breaking point was defined as either a) a maximum height error beyond the 2% or 1.5 feet allowable by ARINC 707, or b) any height reading labeled NCD.

#### 2.4.4 Test Definition

Table 2.6 shows the interference signals used for one of the last runs of the initial testing regimen. This test definition was the result of a year and a half long process of experimentation with the test setup. Tests experimented with loop loss settings, investigated the ARINC429 synchronization issues, investigated the relative sensitivity of different portions of the band, and investigated the bandwidth dependence of interference signals. The results of the earlier tests are summarized here, while the test definition from Table 2.6 is used as a representative example.

Early tests experimented with the position from which loop loss was to be measured. There was an argument that the loop loss should be measured between the terminals of the altitude simulator rather than the terminals of each altimeter. This was abandoned when multiple altimeters were unable to acquire an altitude signal with the higher loop loss. This led to the values from Table 2.1 of attenuation between altimeter terminals being finalized. Investigations into the measurement synchronization issue were covered in depth in Section 2.3.1.3.

Another early test procedure investigated which portion of the radio altimeter band was most sensitive to interference. OFDM signals of the same bandwidth were placed at varying center frequencies to test the altimeters' sensitivity to band placement. These tests confirmed the hypothesis that the center of the radio altimeter band was the most sensitive to interfering signals.

Finally, the test regimen shown in Table 2.6 was used to systematically investigate the sensitivity of the radio altimeters to different bandwidths of interference. These signals were used across all altimeters under test, and across all altitudes the optical delay line could produce in Table 2.1. The results are discussed in Section 3.2.

## **2.5 Expanding the Test Setup**

The results from the initial test regimen led to new avenues of investigation. The dependence of results upon the bandwidth occupied by interference signals led to a need for wider bandwidth signals in the test bed. A desire to present the worst possible case for an aircraft led to testing at lower altitudes with interference from other altimeters. This simulated an approach or takeoff scenario at a busy airport. Finally, developments in 5G communications lobbying for access to adjacent bands led to an investigation of the tolerance of real altimeters to out of band interference. All of this required modifications to the initial testing concept from Figure 2.2 to couple in an extra VSG and simulated altimeter signals at the interference injection point (Figure 2.9).

### **2.5.1 Adding The Second VSG**

Early testing clearly demonstrated the effects of interference bandwidth on the altimeter signal processing. Wider bandwidth OFDM signals caused the altimeter to break at a lower RF Carrier power than narrower bandwidth signals. This dependence made it necessary to demonstrate the effects of OFDM filling the entire 4200 to 4400 MHz band (see Section 3.2 Results of initial testing). However, the Rhode and Schwarz SMU 200A VSG used for initial testing could only support an 100 MHz OFDM signal due to bandwidth limitations on the instrument.

To supplement this, a Rhode and Schwarz SMW 200A was located in the senior design lab, and was appropriated (with permission of the owner) for the purpose of expanding the testing

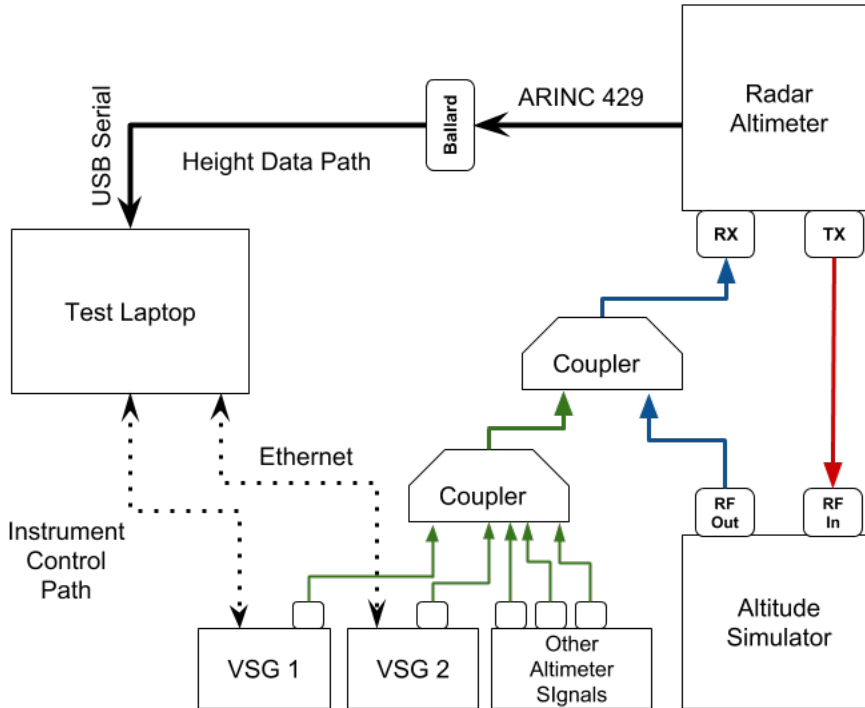


Figure 2.9: Expanded Test Bench For Wideband and Altimeter Interference.

capability. This slightly newer VSG could support a 160 MHz OFDM signal, and when used in conjunction with the first VSG, the two filled the full spectrum. A secondary goal of this process is to test the effects of proposed cellular networks in adjacent bands to the altimeter band while still maintaining simulated WAIC Interference. The dual VSG setup allowed for the one VSG to simulate in band interference while the other swept through out of band signals.

#### 2.5.1.1 Providing Isolation to the VSGs

One problem with using the 6 dB resistive power divider to couple the interference from the two VSGs together was the lack of isolation. The coupler provides no directionality, and signals which enter one port are split equally between the two other ports. This was hazardous since the high interference powers being tested could damage the other VSG if fed into the *RF Out* port in reverse.

AVSI began looking into purchasing other couplers to provide higher isolation to the VSGs, when the Garmin engineer participating in the project offered to contribute two circulators which

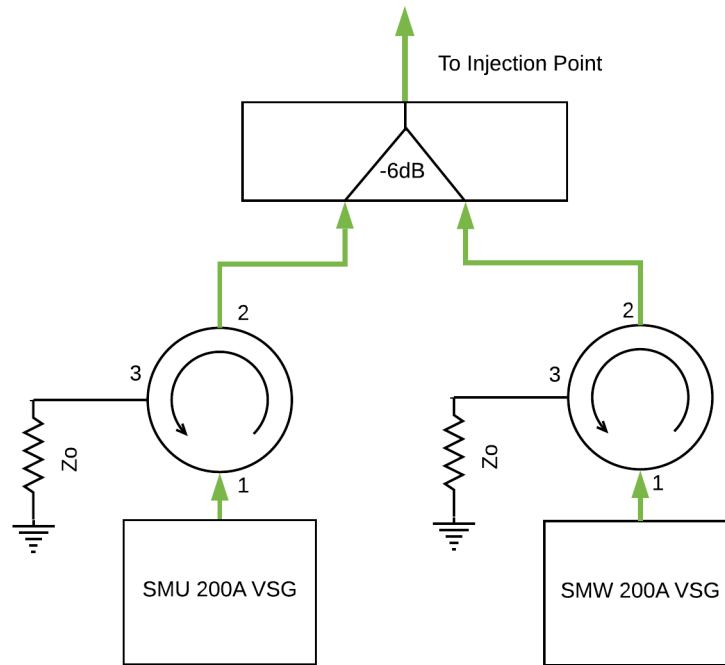


Figure 2.10: Circulator with Matched Load Added to Protect VSGs.

could function as isolators. By placing a matched load at port 3, most power entering from port 2 is absorbed into the load, with very little (ideally none) reflected back to port 2 or allowed to pass to port 1. Signals entering port 1 experience a small attenuation due to the properties of the circulator. Figure 2.10 shows how circulators in this configuration provide isolation to the VSGs when coupled together.

### 2.5.1.2 Achieving Higher Power Interference

The isolators protected the VSGs from damaging each another but they also added more attenuation into the line. This additional loss resulted in the altimeter RX receiving a lower RF power than in earlier tests. This impacted the dynamic range of the Peak Envelope Power (PEP) limitation for the VSGs and prevented tests from locating the breaking point of an altimeter in some cases.

The setup was modified again to fix this. The 20 dB attenuator placed on the output of the optical delay line in the altitude simulator was removed, and the 16 dB directional coupler was

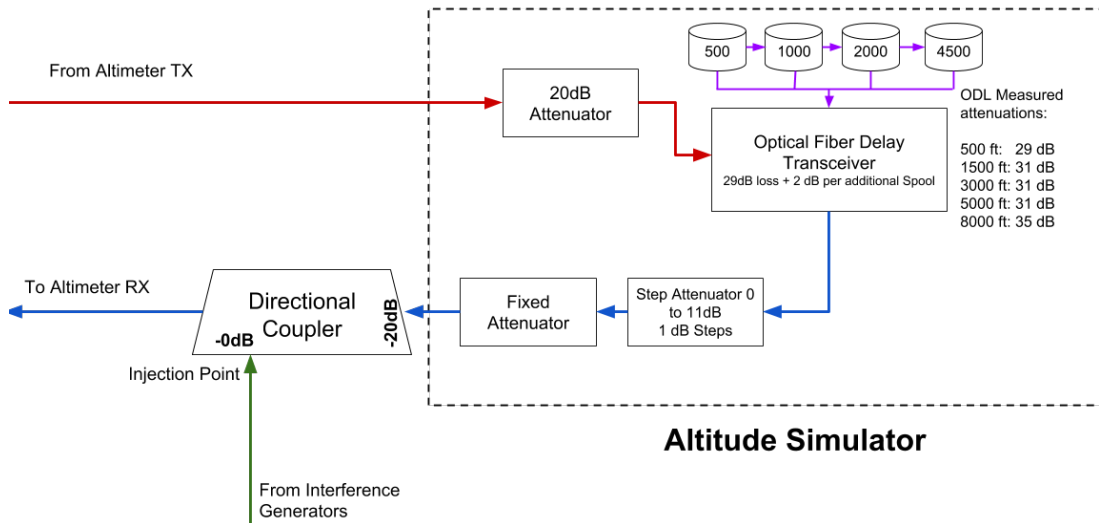


Figure 2.11: Modifications for Higher Interference Power.

replaced with a 20 dB directional coupler. Figure 2.11 shows how the output of the altitude simulator fed into the 20dB loss port of the directional coupler to compensate for removing the fixed attenuator, and the interference injection point was moved to a port with (ideally) no attenuation. Additionally, this configuration was advantageous because the step attenuator and variable fixed attenuator settings for different altitudes did not have to be recalculated.

A Vector Network Analyzer S21 measurement was taken to verify the isolation provided by this configuration, as well as the attenuation between each VSG RF port and the altimeter RX.

### 2.5.2 Simulating Altimeter Interference

The other major modification shown in Figure 2.9 was the addition of other altimeter signals to the interference already being tested. This addition intended to move the setup closer to the real-life worst case scenario for the interference an altimeter might be subjected to. The test bed was configured to replicate an approach for landing scenario used in earlier compatibility investigations. A series of VCOs were calibrated and driven by function generators to generate the external altimeter signals, and programmable and fixed attenuators configured the distance of each altimeter signal from the receiver. The VSG setup was configured to simulate the interference of the full

4.2 to 4.4 GHz band filled with WAIC signals from other aircraft, with a goal of determining what WAIC radiated power limitations were necessary to protect altimeters. Finally, all of these signals were coupled together with the VSG signals to send toward the interference injection point.

### 2.5.2.1 Determining the Worst-Case Scenario Geometry

A worst-case scenario for the interference experienced by a victim altimeter from other aircraft was developed in the 2014 compatibility studies submitted to the ITU [13]. The authors determined that the altimeter data was most important to the safety of a flight during the landing phase of operation. When aircraft line up for approach, they typically maintain a distance of around 5 km, which makes interference from WAIC signals or other altimeters aboard these neighbors negligible. On the other hand, aircraft taxiing or in holding adjacent to a runway can achieve distances less than 300 m to the victim RA. These aircraft could present a significant hazard to nearby altimeter receivers if WAIC power limitations are not developed in the context of this scenario.

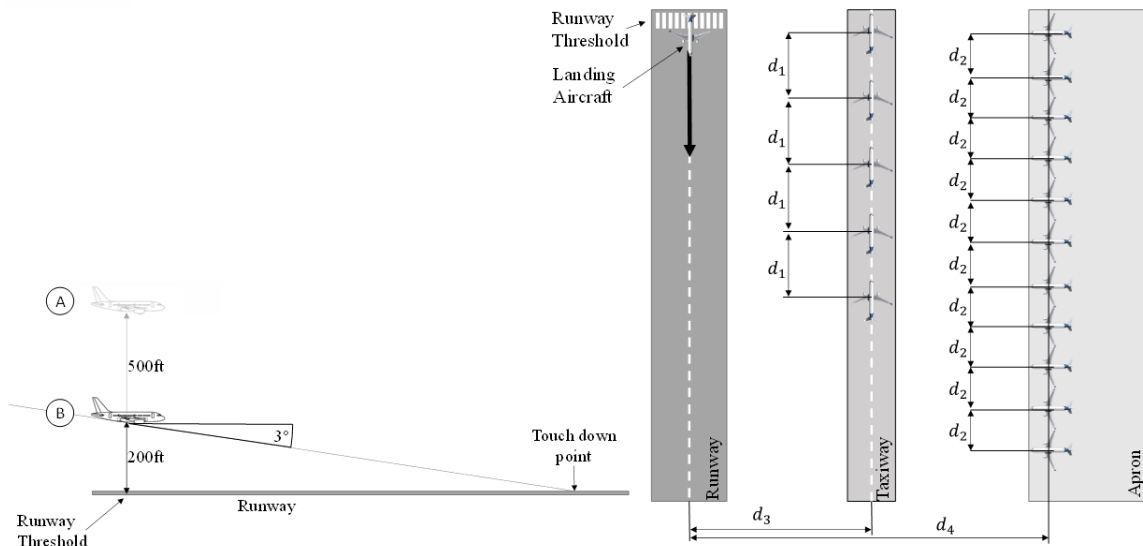


Figure 2.12: Geometry Provided by Project Member Airbus for Landing Scenario.

Figure 2.12 shows the geometry used for this compatibility study. This geometry was developed by project member Airbus based off of the geometry used in previous compatibility stud-

ies [13]. Several parameters specify the distance of aircraft to one another in this scenario. These are the *taxi distance*  $d_1$  between aircraft queuing for takeoff, the *parking distance*,  $d_2$  between parked aircraft, the *ground distances*,  $d_3$  and  $d_4$ , between the runway and adjacent taxiway and hangars respectively. Finally, the *altitude* of the victim aircraft during descent with a 3 deg glide slope determines the victim position along the runway. A *slant range* between the victim RA and an interferer can be determined using these parameters.

The path losses from simulated WAIC signals were calculated in the context of this geometry. Altimeter transmitters and receivers were located at the center of the airframe, directly underneath each aircraft. Interferers modeling all WAIC devices were grouped together at the center-point inside of each airframe. The WAIC system was modeled as an isotropic radiator in this location for each aircraft.

In addition to specifying the path loss experienced by WAIC interferers, this geometry also served to model the interference subjected to the victim RA by other altimeters. Most altimeters are designed to handle external altimeter signals, but the *combination* of these signals with WAIC interference leads to more stress on the victim receiver. This geometry models the locations of external altimeters along with WAIC signals to simulate this effect, allowing for a single ground bounce from interferer transmit antenna to victim receive. Multipath was not modeled in this scenario which serves as one of the limitations of this analysis. Path losses assigned to each simulated altimeter are specified by the location in this geometry.

The geometry was then modeled in a Matlab script by Airbus as a contribution to this project. The victim aircraft approached for a landing on a 3 degree glide slope, and the interference path loss (IPL) from each aircraft on adjacent taxiways were modeled in the script. Figure 2.13 shows the results of this analysis. The IPL value for each of the 15 nearest aircraft are shown as a function of height, with a minimum occurring at approximately 200 ft due to the angle of reflected interference signals offering the shortest direct path into the victim RX antenna. From this, the committee drew the conclusion that the worst case altitude for this geometry occurred at approximately 200 ft.

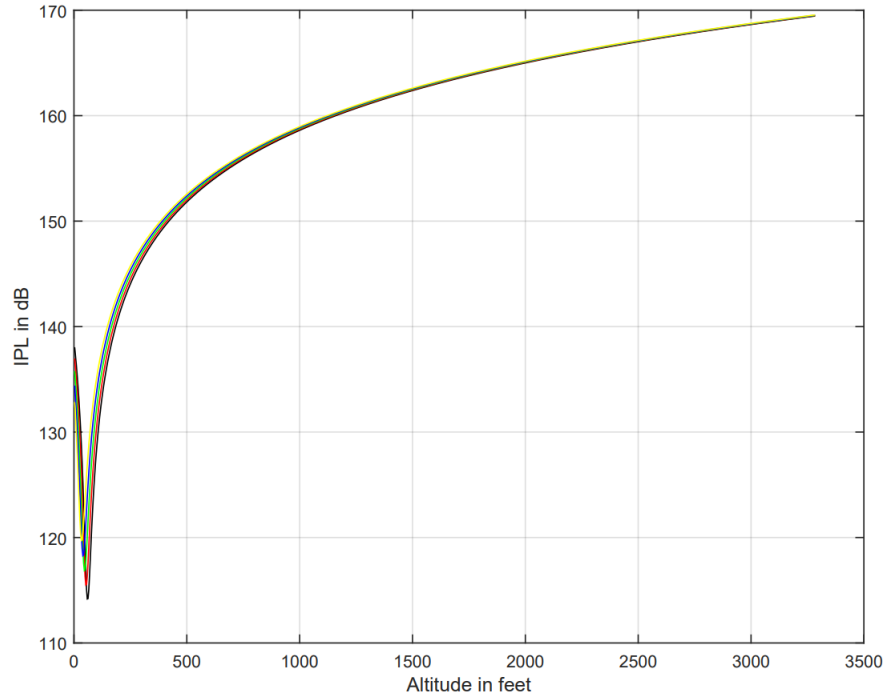


Figure 2.13: Plot of IPL Values for 15 Closest Aircraft

However, the lab test equipment had available test altitudes of only 40 and 500 ft. After some deliberation, the 500 ft altitude was chosen for the approach tests. By configuring the IPLs for the 200 ft case, and the altimeter loop loss for a 500 ft case, the signal to interference ratio went from the real life worst case scenario to a so-called ‘super’ worst case scenario:

$$\frac{S(200ft)}{I(200ft)} \leq \frac{S(500ft)}{I(200ft)}.$$

This super worst case would be used to configure interfering altimeters for the landing simulation.

#### 2.5.2.2 *Simulating Individual Altimeter Signals*

Several approaches were considered to simulate altimeter signals for the approach scenario. Software defined radios were appealing for the convenience they offered in modifying the test bed. Despite this advantage, they were rejected in favor of a series of Voltage Controlled Oscillators (VCOs) controlled by function generators. The major advantage seen in the VCO approach was

the simplicity of explaining the test scenario to regulators, as opposed to having to present another piece of software.

Eight two-channel function generators and 16 VCOs were ordered for this purpose. The function generators were configured to output a triangle voltage wave to drive the VCOs in the FMCW pattern seen in Figure 1.1. The min and max voltage on the triangle wave correspond to the VCO setting for the min and max frequency of the simulated altimeter waveform. The frequency of the voltage waveforms was varied between different VCOs to simulate the varying pulse frequencies exhibited by different altimeters as well as to provide randomness to the simulation. It was considered critical that the different simulated altimeter signals were asynchronous to provide a realistic scenario.

### 2.5.2.3 Connecting the VCO Signals

Figure 2.14 shows how the VCO signals were coupled together to simulate 16 different altimeter signals. The initial plan had been to simulate every altimeter on the 15 closest aircraft to the victim. However, the VCOs became backordered after the first 16, and empirical studies showed that the effects of the higher power “on board” simulated altimeter signals overwhelmingly dominated the effects of the “external” VCOs. Each VCO was configured to simulate the RF power of

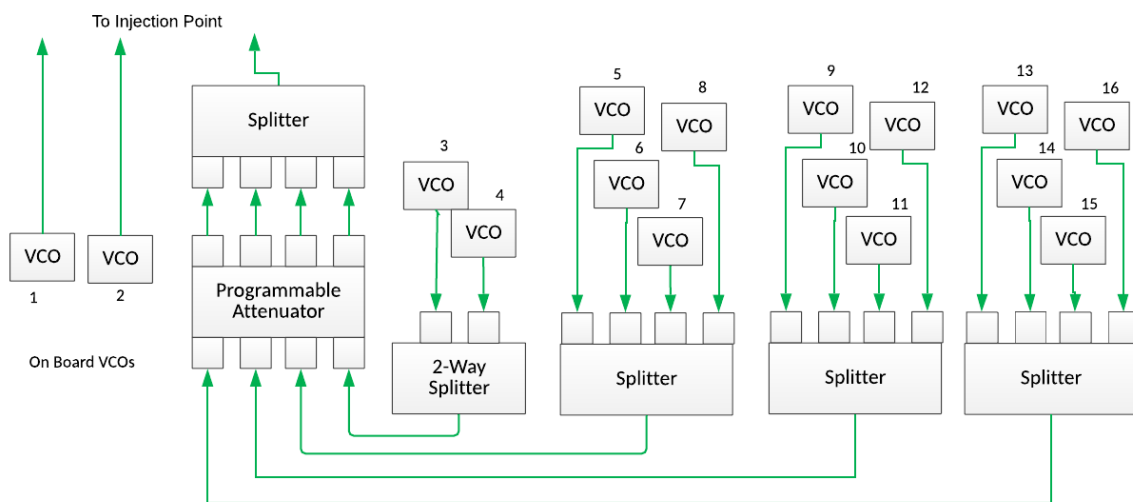


Figure 2.14: Diagram of Combined 16 Simulated Altimeter Signals.

VCO	Power [dBm]	Fixed [dB]	Programmable [dB]	Path Loss [dB]	Power at RX
<b>1</b>	4	-18	X	-16	-30 dBm
<b>2</b>	4	-18	X	-16	-30 dBm
<b>3</b>	4	0	-56	-40	-92 dBm
<b>4</b>	4	0	-56	-40	-92 dBm
<b>5</b>	4	0	-26	-40	-62 dBm
<b>6</b>	4	0	-26	-40	-62 dBm
<b>7</b>	4	0	-26	-40	-62 dBm
<b>8</b>	4	0	-26	-40	-62 dBm
<b>9</b>	4	0	-26	-40	-62 dBm
<b>10</b>	4	0	-26	-40	-62 dBm
<b>11</b>	4	-23	-26	-40	-85 dBm
<b>12</b>	4	-23	-26	-40	-85 dBm
<b>13</b>	4	0	-49	-40	-85 dBm
<b>14</b>	4	0	-49	-40	-85 dBm
<b>15</b>	4	0	-49	-40	-85 dBm
<b>16</b>	4	0	-49	-40	-85 dBm

Table 2.7: VCO Attenuation Configurations for 200ft Worst Case.

an altimeter (typically 30 dBm), and the associated path loss from interferer TX to victim RX. This was accomplished with a variety of sources of attenuation. Each VCO output 4 dBm of RF power according to the data-sheet. Fixed attenuators could be placed at the RF output of each VCO to achieve individualized IPL values. Each splitter contributed 6 dB of attenuation to a connected path. The 4-channel programmable attenuator offered programmable values between 0 and 63 dB of attenuation. Lab measurements found that the programmable attenuator contributed 4 dB with a programmed setting of 0 and confirmed that each dB of programmed attenuation added one dB to this value. Finally, the attenuation from the interference injection point to the altimeter RX is added to the path loss.

#### 2.5.2.4 *Calibrating the VCOs*

The VCOs ordered for this purpose could go beyond the 4.2-4.4 GHz range, but a control voltage did not necessarily map to the same frequency across different VCOs. This meant that each of the 16 VCOs needed to be calibrated. First, each VCO was connected to a 5V power supply, and the control pin was connected to a separate power supply. The RF output of each VCO

VCO	Lower		Upper		Function Generator Setting		
	Voltage	Freq [GHz]	Voltage	Freq [GHz]	Center	Amplitude	Freq [Hz]
1	2.2	4.237	4.0	4.362	3.1	1.8	143
2	1.6	4.236	3.5	4.367	2.6	1.9	143
3	2.2	4.232	4.1	4.365	3.2	1.9	143
4	2.0	4.233	3.9	4.364	3.0	1.9	111
5	1.8	4.233	3.7	4.364	2.8	1.9	133
6	2.0	4.238	3.8	4.362	2.9	1.8	133
7	1.8	4.233	3.7	4.365	2.8	1.9	133
8	1.7	4.233	3.6	4.368	2.7	1.9	118
9	2.0	4.235	3.9	4.367	3.0	1.9	118
10	2.0	4.233	3.9	4.365	3.0	1.9	118
11	2.0	4.238	3.8	4.362	2.9	1.8	111
12	2.1	4.236	3.8	4.366	3.0	1.7	129
13	1.8	4.235	3.7	4.364	2.8	1.9	129
14	2.0	4.235	3.7	4.366	2.9	1.7	129
15	2.1	4.237	3.8	4.368	3.0	1.7	143
16	2.3	4.233	4.2	4.365	3.3	1.9	143

Table 2.8: VCO Calibration Results and Corresponding Function Generator Settings.

was connected to the spectrum analyzer for observation. The frequency output by a VCO under constant voltage had a bit of a ‘wobble’ to it, so the spectrum analyzer was configured to display a *Max Hold* instead of a real time measurement. After a VCO was left on a control voltage for several seconds, a marker was used to locate the frequency of the maximum output at that setting.

The first calibration sweep went from 0 to 5 V in 1 V increments. The goal of this broad sweep was to get an approximation for where the 4.2 and 4.4 GHz voltages were for each VCO. The VCO output was observed on the spectrum analyzer to determine the operating frequency at that control voltage. The search found that a majority of the 4.2–4.4 GHz band lied in the 2–5 V range for these VCOs. The initial sweep was not fine enough to capture the desired minimum and maximum frequencies for each VCO.

A second calibration was attempted to fix this. The goal was to get the simulated FMCW waveforms centered at 4.3 GHz, with a span of  $\pm 65$  MHz. Using 100 mV increments, the previous calibration procedure was repeated, this time explicitly searching for the control voltages

corresponding to the frequencies closest to 4235 MHz and 4365 MHz. These were achieved with a  $\pm 3$  MHz precision. The 100 mV increments from the calibration process were chosen due to the precision available to the function generators. It was this limitation that led to the 3 MHz frequency precision. The full calibration results are shown in Table 2.8.

Once the lower and upper voltages were determined, a simple calculation found the center voltage and amplitude necessary to feed into the function generators. In addition to the amplitude and offset settings available to the function generator, the control voltage wave had a frequency parameter. These were chosen in part with enough variance so that there was no synchronization between the different simulated altimeter signals. Random crossover of the simulated altimeter signals was desired to closely match the real world interference scenario. Function generator parameters are also shown in Table 2.8.

#### 2.5.2.5 VCO Protection Circuit

The VCOs were designed to operate with a control voltage between 0 and 5 V. They were found experimentally to tolerate a maximum voltage of 6.5 V before catastrophic failure but the function generators were capable of outputting up to 20 V peak-to-peak. This created a need to provide protective circuitry for the VCO that could mitigate the possibility of damage to the device.

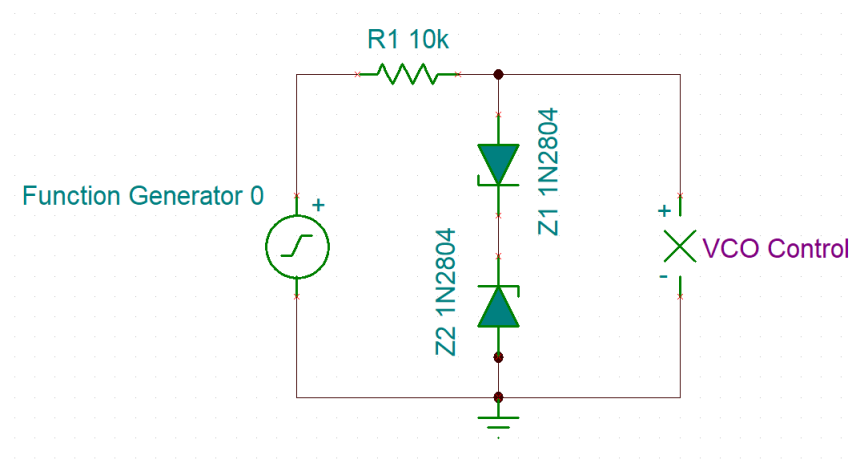


Figure 2.15: Double Clipper Protective Circuit.

Initially, the protective circuit seemed even more urgent. The voltage setting on the function generator starts at 10 V upon power up, but does not clearly mark whether this is a peak to peak voltage or  $\pm 10$  V. Compounding this ambiguity, when the output of the function generators was measured with an oscilloscope, the multiplier setting was set to 2X. This made it appear to be a  $\pm 10$  V signal on startup which would fry the VCO if the function generator was accidentally power cycled. This error was only noticed after the protective circuit was designed and built.

After some searching, a limiter or ‘clipper’ circuit was decided on to protect the VCOs. Clippers consist of a resistor and one or two diodes. Various designs of clipper circuits and the trade-offs between them are discussed in [14]. Based on this discussion, a double clipper like the one shown in Figure 2.15 was decided on. Two Zener diodes begin to limit the upper and lower voltage extremes once they pass the diode’s cutoff voltage. A resistor is placed in series with the diodes to limit the current in the diodes to safe levels.

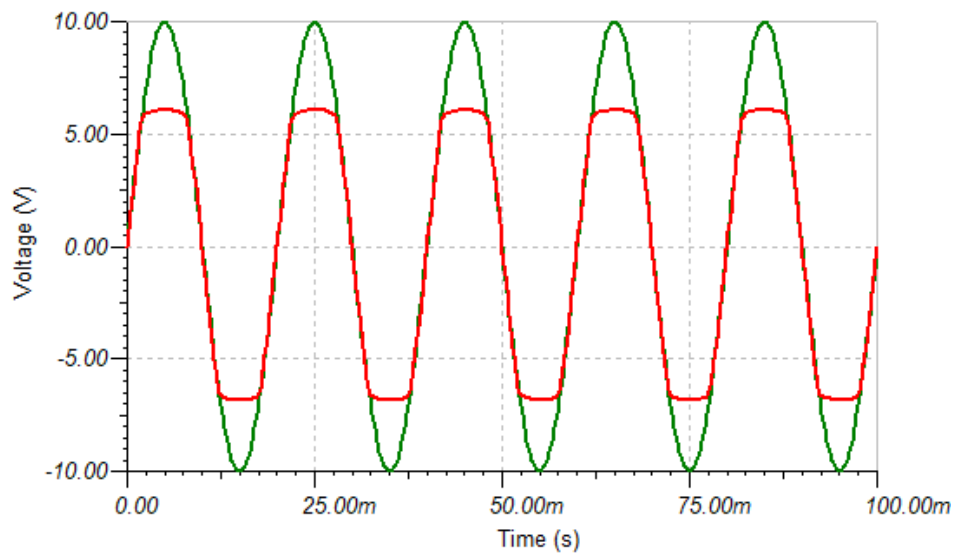


Figure 2.16: Clipped Sin Wave.

The clipper circuit was modeled in a spice program so that different diode cutoff voltages could be tried. Simulations showed that the output voltage from this circuit would typically go slightly

above the cutoff voltage. Because of this, a Zener diode with a 6 V cutoff was chosen to limit the output below the 6.5 V failure point. A simulated output from the clipper circuit waveform is shown in Figure 2.16. A  $\pm 10$  V sine wave is fed from the function generator, shown in green, and the ‘clipped’ waveform is shown in red. The circuit allows voltages close to the failure point without reaching it. This performance was verified with an oscilloscope for each function generator output.

### 2.5.3 Testing Lower Altitudes

A final major modification from the initial test regimen involved adding different altitude simulator configurations to the rotation to achieve lower altitudes. These were touched on briefly in Section 2.2.2. Lower altitude tests were first started before the approach scenario analysis determined that 200 ft was the worst case scenario. Once the worst case analysis was determined, lower altitude tests were continued to provide supplementary evidence at another altitude in the landing scenario.

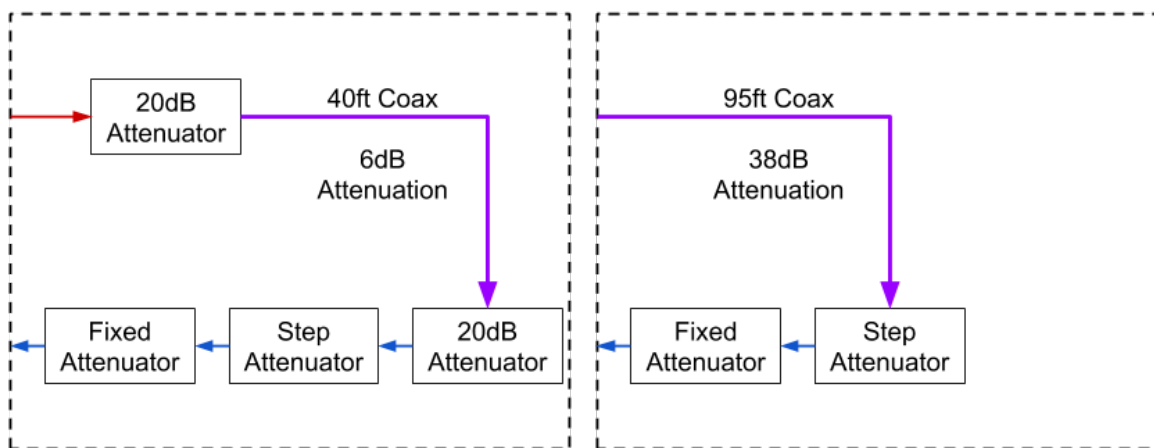


Figure 2.17: Left: 40ft Altitude Simulator; Right: 95 ft Altitude Simulator.

Two different coaxial cables were used to simulate different altitudes below the 500 ft threshold the optical delay line was capable of. Firstly, a coaxial cable providing 40 ft altitude was located in the lab for this purpose, shown on the left of Figure 2.17. When measured with a VNA, this coax

had only a 6 dB attenuation, so two 20 dB fixed attenuators were placed on either side to increase the attenuation. This allowed the same step and fixed attenuator combination from Figure 2.3 to easily achieve the DO-155 attenuation from Table 2.1. The 40 ft altitude simulator underwent the same modification as the Fiber Optic Line in Figure 2.11, which allowed higher power interference signals without modifying the fixed and step attenuator settings in use.

The second altitude simulator used during these tests was a 95 ft cable which was ordered after a significant number of 40 ft tests had been run. The 40 ft tests had revealed a problem where one of the newer altimeters (with more advanced signal processing) would not output an altitude below a certain threshold unless it detected that the aircraft was moving. This precipitated the 95 ft tests so that an altitude below the 200 ft worst case could be tested across all units. The 95ft cable was a lower quality coax than the 40 ft cable, and when measured with a network analyzer showed an approximately 38 dB attenuation at 4.3 GHz. This was confirmed to be approximately the expected attenuation for this length of coax from the manufacturer's website. Once again, a fixed and step attenuator allowed the altitude simulator to be fully adjustable and achieve the DO-155 specified attenuation.

## **2.6 Expanded Setup Test Plans**

The different modifications discussed above were combined into a full setup. This was used to test the altimeters in approach scenarios, to determine a breaking point for full spectrum interference for the purposes of regulation, and to investigate the effects of adjacent band interference signals.

### **2.6.1 Full Setup Diagram**

Figure 2.18 shows the full test setup diagram. The modifications covered in Section 2.5, including the second VSG, isolators to protect the VSG's, and the VCO setup to simulate 16 other altimeter signals are included in this diagram. Depending on the desired test scenario, the lower altitude simulators from Figure 2.17 were substituted in for the optical delay line, and as tests progressed, the modification shown in Figure 2.11 allowed for higher interference powers.



Interference Signal			VSG RF Power			Power Durations	
Modulation	Bandwidth	Center	Min	Step	Max	ON	OFF
OFDM	200 MHz	4300 MHz	-56 dBm	2 dB	19 dBm	60 s	20 s

Table 2.9: Example Interference Signals for Wideband Testing.

Interference Signal				VSG RF Power			Durations	
Modulation	Bandwidth	Center Frequencies		Min	Step	Max	ON	OFF
		Min [MHz]	Max [MHz]					
OFDM	200 kHz	3900	4200	-14 dBm	2 dB	18 dBm	10 s	5 s
OFDM	200 kHz	4400	4700	-14 dBm	2 dB	18 dBm	10 s	5 s

Table 2.10: Example Interference Signals For Out Of Band Testing.

interference signals under worse than possible real life conditions. When the worst breaking point among the altimeters sampled was found, the committee would add a margin of a few dB and propose that number to regulators. These results are discussed in Section 3.3

#### 2.6.4 Out of Band Testing

Finally, Table 2.10 shows a representative test definition for the out of band tests run under AFE76s2. These tests were designed to develop an RF power mask on the upper and lower side of the radio altimeter bands. This mask could be brought to regulators with a proposal to limit users in adjacent bands a certain margin below the altimeter breaking point.

Initially, the 5 MHz wide OFDM signals used in previous tests were tried. However, after initial results came in, more granular sweep was desired, so the bandwidth was reduced to the 200 kHz signals shown in Table 2.10. When the 200 kHz waveform was measured on the spectrum analyzer, it was noticed that the waveform center was slightly offset from the carrier frequency. The lower edge of the waveform was approximately 35 kHz below the carrier, and the upper edge was approximately 165 kHz above the carrier.

Since the test goal was to step an OFDM waveform with the upper edge directly on 4.2 GHz, and step away from the altimeter band till the upper edge was 5 MHz away from the band edge.

Waveforms in the upper adjacent band were placed at 4200.035 MHz and stepped to 4205.035 MHz for the same reason.

These tests are ongoing at the time of writing, and will likely go through a few more iterations before being finalized, but preliminary results from this test definition are discussed in Section 3.4.

## 3. RESULTS

The radio altimeter tests described in this work were developed over a two year long process which can be approximately separated into three distinct phases of testing. The initial testing results discussed in Section 3.2 characterized the basic response of altimeters to various types of interference. These led to another set of tests aimed at more systematically demonstrating altimeter performance under more conservative than real life conditions. The in-band testing in Section 3.3 demonstrated what power level of a full 200 MHz of WAIC interferers would break an altimeter in the worst case scenario. Finally, the Out of Band testing regimen investigated altimeter performance when subjected to cellular interference in neighboring bands. Preliminary out of band results are discussed in Section 3.4. Results of the two later testing regimens were used to propose maximum radiated power values to regulators, as well as in continuing discussions.

### 3.1 General Plotting Scripts

This setup introduces the two general types of plots used across all tests, called ‘Height Plots’ and ‘Stat Plots’ respectively. The form of these was evolved over the course of different testing regimens to communicate the results from each effectively, but the basic plots introduce a standard format in which results from an altimeter test are displayed.

#### 3.1.1 Height Plots

The first attempts at a representation of data taken during these tests developed into *height plots*. The goal of the height plot is to provide a visualization of how the interference signals from the VSG distort the altitude signal output by an altimeter over time. In each altimeter test, a height plot is generated for each unique combination of center frequency and modulation format under test. Figure 3.1 shows an height plot from the initial testing regimen.

Important information about the test being displayed is contained in the title of each height plot. This includes the altimeter make and model, the bandwidth and modulation format of the interference signal being tested, and the center frequency of RF carrier setting used by the VSG.

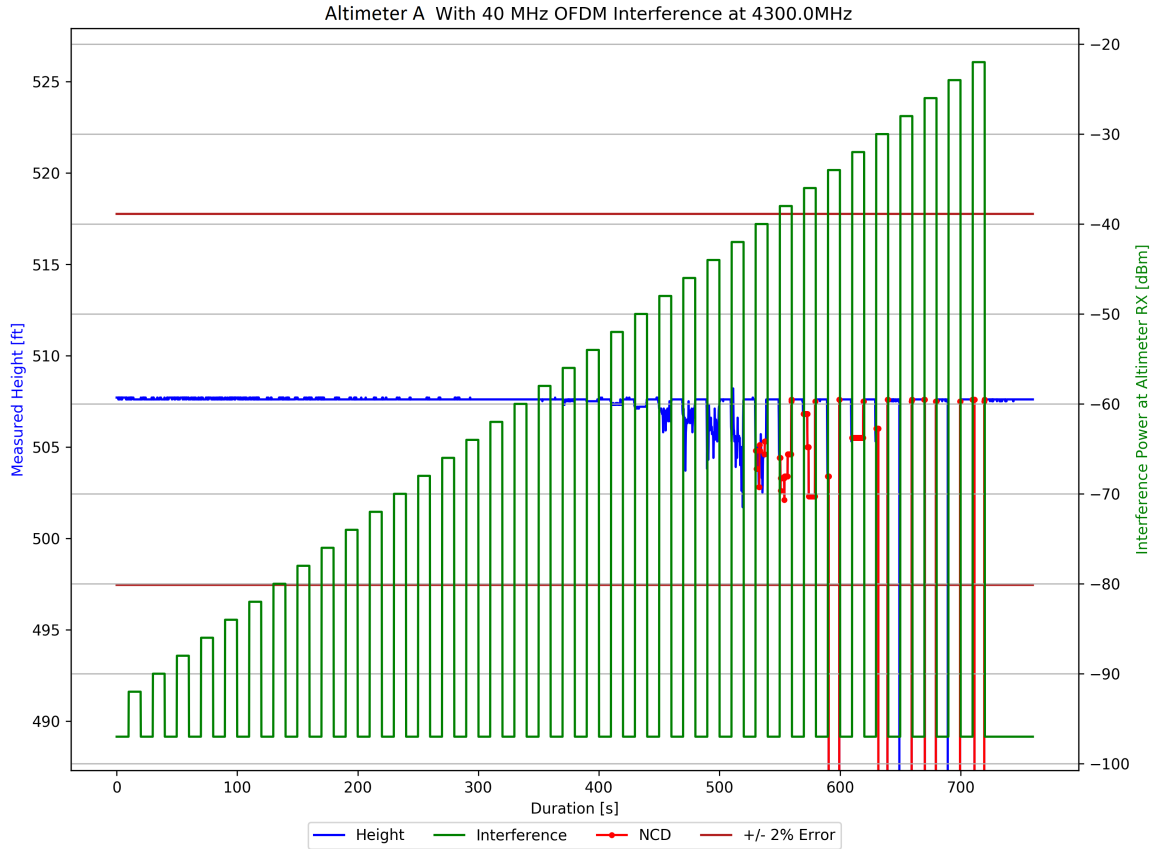


Figure 3.1: Example Height Plot from Initial Testing Regimen.

The  $x$ -axis shows the test duration in seconds. After the SQL query sorts by modulation and carrier, the zero second point is set to correspond to the start time for the first RF OFF state for the first interference signal. This time-stamp is subtracted from every mapped data point to yield a plot vs test duration in seconds.

The left hand  $y$ -axis shows the height output by an altimeter in feet. The axis is centered about *correct height* calculated as the median height before any interference is turned on (See Section 2.3.1.1). The upper and lower bounds of this axis correspond to  $\pm 4\%$  error from this correct height respectively. The height signal is plotted with a blue line, but for measurements labeled NCD by the device under test, this is replaced with a bright red marker to clearly show the failure state. Finally, the burgundy lines show the ARINC 707 specified  $\pm 2\%$  error margins. Measurements passing this value constitute a device no longer meeting specifications for certification and

are considered severe.

Finally, the right hand  $y$ -axis corresponds to the interference power level experienced by the altimeter receiver. The green staircase waveform shows how the RF generator was toggled on and off in increasing power levels over time. To easily signal an OFF state, the OFF state was plotted on the same line as the ON state, with 5 dB subtracted from the minimum interference power used in a test.

Displaying the data in height plots has numerous advantages. This format clearly shows how an altitude signal is distorted with increasing interference power over time, as well as how quickly the altimeter recovers once the interference is turned off. This format also allows the point in time an altimeter outputs NCD to easily be located. The plots versus time were extremely useful in debugging a test. Errors such as an altimeter which stops outputting data in the middle of a test manifest themselves clearly in a height plot, and manufacturers can correlate this data with recordings of the internal signal processing data stored on SD cards during a test.

### 3.1.2 Stat Plots

Despite the advantages stated above, height plots had a disadvantage of being extremely cluttered. When presenting test results to regulators, members of the project management committee tended to spend a disproportionate amount of time discussing the different aspects of the data display as opposed to the results themselves. This motivated the development of stat plots.

Figure 3.2 shows an example stat plot made from the same data as the Height Plot in Figure 3.1. Stat plots show height error from the correct height versus RF power at the altimeter receiver when the RF power is on. The mean, max, and min are all plotted along with standard deviation error bars and a marker to indicate NCD. Because the noise caused by interference power is not necessarily a normal distribution, the standard deviation error bars do not necessarily have the precise meaning they do with Gaussian noise. However, the error bars do provide a visual representation for how much variance from the mean a given RF power causes. Because of this, they are kept in the plot as a good way to communicate the data.

Although stat plots do not contain any information about the timing of different events in an

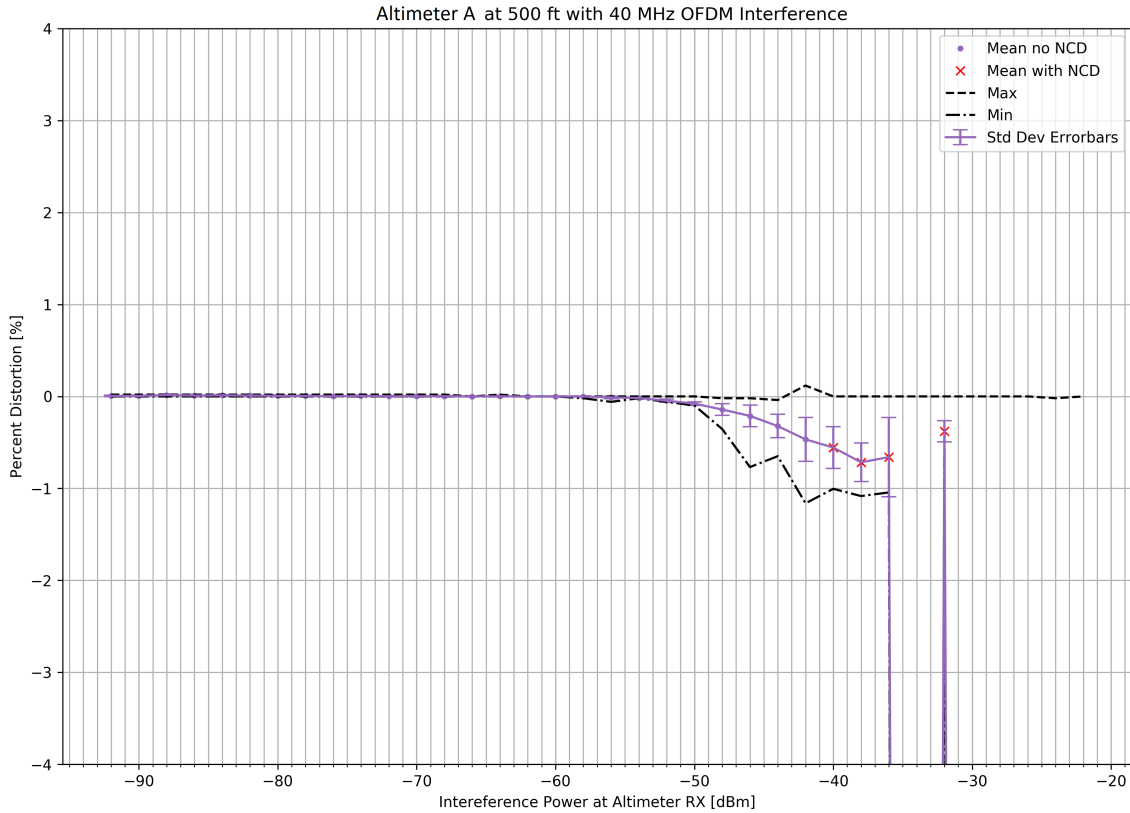


Figure 3.2: Example Stat Plot.

altimeter test, they provide a more concise and clean method to display the results of an altimeter test. These features led this representation to be used to communicate test results in letters to the International Civil Aviation Organization (ICAO) Frequency Spectrum Management Panel (FSMP) [?].

### 3.2 Initial ‘WAIC Only’ Testing Regimen

This section covers the results of the initial testing regimen described in Section 2.4. The ‘WAIC only’ testing was a long term, multifaceted investigation which characterized various aspects of the altimeter response to interference. The test definition from Table 2.6 shows a representative example of a test run with a single altimeter. This would be repeated for the 5 different commercial altimeters sampled for these tests, and for each height the test setup was capable of.

Figure 3.3 shows a comprehensive summary of these results. Each data point on shows the

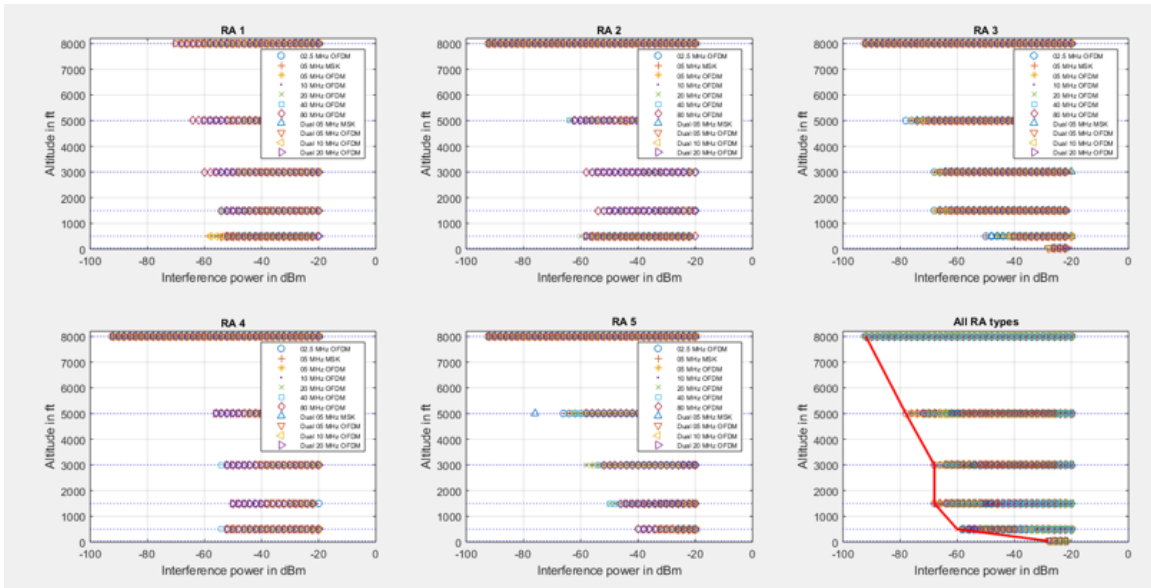


Figure 3.3: Summary of Initial Testing Results

results of a single altimeter test equivalent to a height plot in Figure 3.1. The data points plot the power level at which the altimeter under test goes beyond a mean error of  $\pm 0.5\%$ . This plot served as an introduction to the presentation of the results of the second and third testing regimens [?], as a means of showing how the WAIC only tests justified further investigation.

Early tests investigated the proper loop loss value to use. Although loop losses were specified in DO-155 (see Section 2.2.2.2), it was ambiguous as to whether the loop losses were to be measured between the ports of the altimeter or between the ports of the altitude simulator. The language in the regulations made it seem intuitive to place the loop loss between the ports of the altitude simulator. However, when tests were attempted with this configuration, the additional cable loss leading to and from the simulator made the altimeters unable to function. It was hypothesized that the worst case scattering coefficients in use for the loop loss calculation made the addition of cabling turn an already conservative case to an unrealistic one. Because these units were all certified, the loop loss was moved to the ports of the altitude simulator to ensure functionality, and this was noted in any communication of results to outside parties.

A series of tests during the initial testing regimen placed a 10 MHz OFDM signal at different

points in the altimeter band. These showed that the altimeter under test consistently broke at lower power levels when interference was injected at the center of the band than at the outer edges. Subsequent testing only centered simulated WAIC waveforms at the center of the band to provide the most conservative results. Finally, these tests investigated the effects of interference bandwidth on

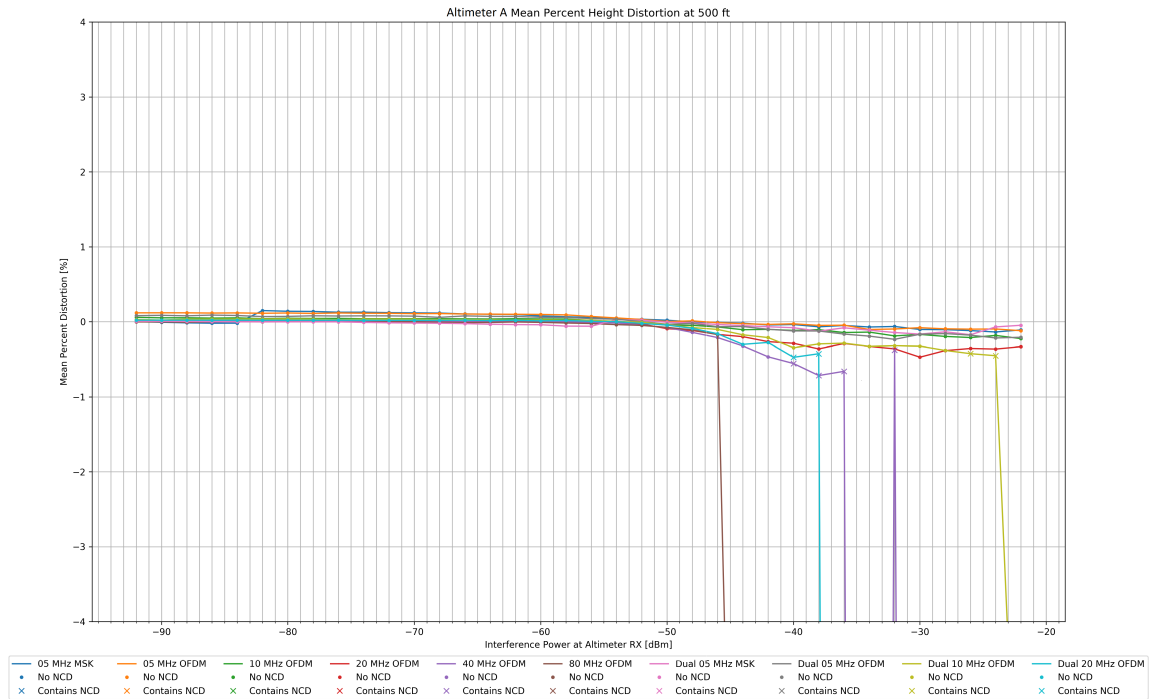


Figure 3.4: Comparison of Impact of Different Bandwidths of Simulated WAIC Signals on Altimeter Performance.

altimeter performance, and the effects of separating a waveform into a ‘dual’ version of the waveform with a  $\pm 20$  MHz offset from the center. The test definition shown in Table 2.6 was the last iteration of the test procedure run before expanding the setup, and functions to demonstrate these effects. Figure 3.4 shows a stat plot comparing the mean height error caused by interference signals of increasing bandwidth. These results consistently showed that wider bandwidth interference caused worse altimeter performance. Although dual waveforms helped performance, their impact was inconsistent.

These results were used to justify expanding the test setup and measuring altimeter response to wider bandwidth WAIC signals aggregated with interference from other altimeters to provide a realistic worst case scenario.

### 3.3 Expanded In Band Tests

This section discusses the results of the testing regimen described in Section 2.6.3. The goal of this iteration of tests was to measure the response of altimeters to a full band of simulated WAIC interference, in the presence of simulated interference from other altimeters. The combined interference represented a more conservative than the real life worse case scenario for altimeter interference. Five different altimeters were tested: the Rockwell Collins LRA2100, The Rockwell Collins LRA900, the Thales ERT530, the Thales ERT550, and the Honeywell ALA52B.

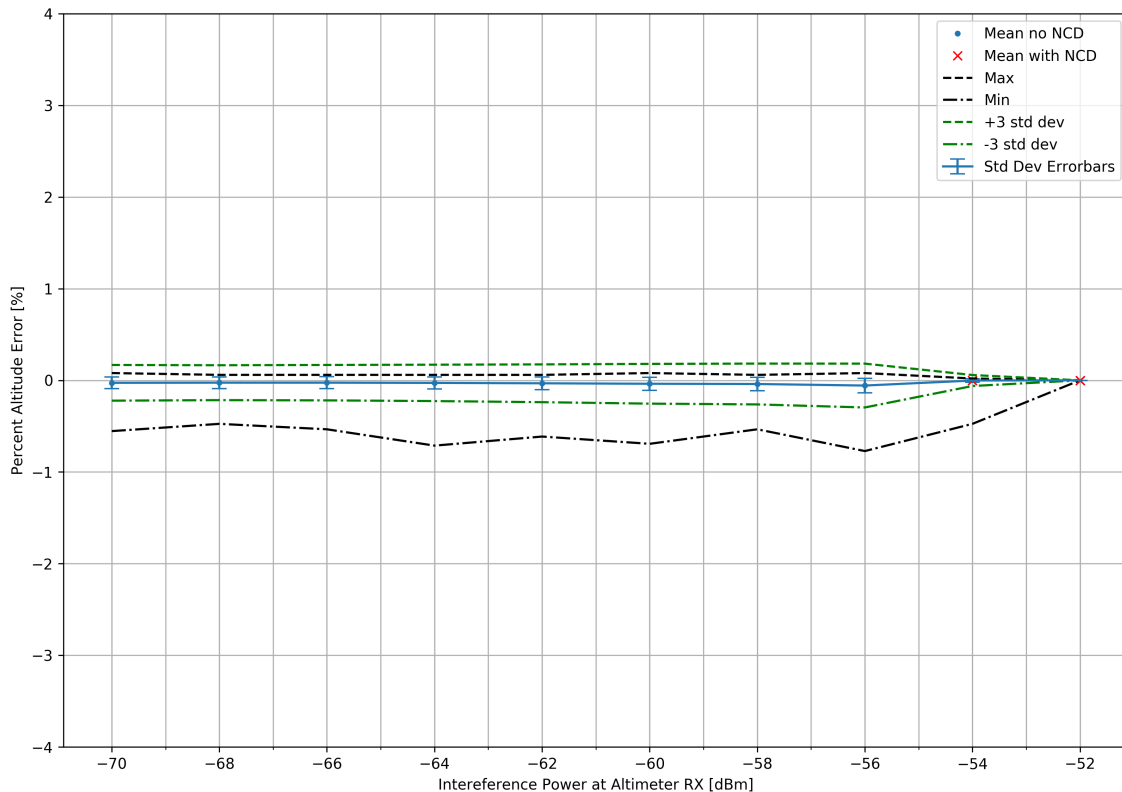


Figure 3.5: Results from RA Type 4 with 200MHz In Band Tests.

	RA Type 1	RA Type 2	RA Type 3	RA Type 4	RA Type 5
WAIC Interference Threshold	-54 dBm	-56 dBm	-44 dBm	-56 dBm*	-44 dBm

Table 3.1: Interference Power Level Above Which Reported Altitude is Impacted [?].

The breaking point of each was found according to Section 2.6.2, and these were used to propose maximum radiated power thresholds to the FSMP [?]. The resulting minimum power thresholds, with altimeter names redacted, are shown in Table 3.1. RA Type 4 performed the worst of the five models tested, so the final threshold recommended to the FSMP was 56 dBm based on this failure point. Figure 3.5 shows the results of this altimeter. The first breaking point occurs at -54 dBm interference power at the altimeter receiver, thus the WAIC threshold was set at -56 dBm. The results of the remaining altimeters are shown in Appendix A for completeness.

### 3.4 Out of Band Testing

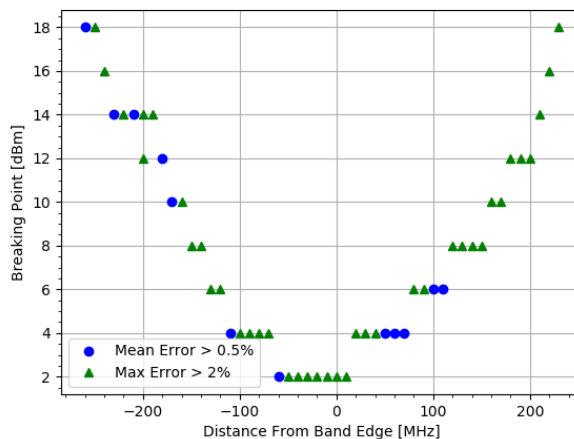


Figure 3.6: Preliminary Interference Mask.

This section covers the results of the out of band testing regimen described in Section 2.6.4. This test used the same expanded test setup as the 200 MHz in-band tests. VCOs were used to

simulate external altimeter signals at a 200 ft approach, and one of the VSG's generated 130 MHz wide simulated WAIC interference. The second VSG stepped RF signals out from the band edges. The goal was to find how the breaking point changed with distance from the band edge in MHz. An example of these results plotted is shown in Figure 3.6. These tests are still in progress at the time of writing, but like the results in Section 3.3, are expected to justify recommendations made to regulators for safe power thresholds in the adjacent bands.

#### 4. CONCLUSION

This work covered the development of a reference test bed for radio altimeter interference susceptibility testing which was validated by altimeter manufacturers and aircraft manufacturers. The test bed was automated in a modular framework which allowed rapid modification to enable testing under a wide range of conditions. Finally, this work covers the support the author gave to the execution, and analysis of data from radio altimeter tests.

The reporting formats created supported the development of international standards for wireless avionics. These include: the International Civil Aviation Organization Standard and Recommended Practices (ICAO SARPs), RTCA inc. Minimum Aviation System Performance Standards (RTCA MASPS), and Minimum Operational Performance Standards (RTCA MOPS). In the future, the wireless avionics equipment governed by these standards will allow air travel to become safer, more fuel efficient, and more economical.

## REFERENCES

- [1] D. Redman, "WAIC Overview and Application Examples," 2011.
- [2] H. Canaday, "War on wiring," *Aerospace America*, May 2017.
- [3] Ferrell, "Feasibility of Intra-Aircraft Wireless Sensors," Final Report AFE 56, Aerospace Vehicle Systems Institute (AVSI), May 2007.
- [4] A. Tewfik, M. Heimdahl, N. Hopper, and K. Yongdae, "University of Minnesota Final Report," AFE 56s1 Final Report, University of Minnesota, Minneapolis, Minnesota, Mar. 2009.
- [5] "Consideration of regulatory actions, including allocations, to support Wireless Avionics Intra-Communications," Resolution 423, World Radio Conference, Geneva, Switzerland, 2012.
- [6] "Consideration of the Aeronautical Mobile (route), Aeronautical Mobile, and Aeronautical Radionavigation Services Allocations to Accommodate Wireless Avionics Intra-Communication," ITU Recommendation ITU-R M.2318-0, International Telecommunication Union, Geneva, Switzerland, Nov. 2014.
- [7] "Final Acts of the World Radiocommunication Conference," Final Acts WRC-15, International Telecommunication Union, Geneva, Switzerland, 2015.
- [8] "Operational And Technical Characteristics and Protection Criteria of Radio Altimeters Utilizing the Band 4 200 - 4 400 MHz," ITU Recommendation ITU-R M.2059-0, International Telecommunication Union, Geneva, Switzerland, Feb. 2014.
- [9] "Minimum Performance Standards Airborne Low-Range Radar Altimeters," Industry Standard DO-155, Radio Technical Commission for Aeronautics, Washington, D.C., Nov. 1974.
- [10] J. G. Proakis and M. Salehi, *Communication Systems Engineering*. Upper Saddle River, New Jersey: Prentice Hall, second ed., 2002.

- [11] “Overview of IRIG-B Time Code Standard,” Technical Note IRIG Standard 200-04, Cyber Sciences, Murfreesboro, TN, Sept. 2017.
- [12] “ARINC Characteristic 707-7 Radio Altimeter,” Industry Standard 707-7, Aeronautical Radio, Inc, Annapolis, Maryland, Apr. 2009.
- [13] “Compatibility Analysis Between Wireless Avionics Intra-Communication Systems and Systems in the Existing Services in the Frequency Band 4 200-4 400 MHz,” ITU Recommendation ITU-R M.2319-0, International Telecommunication Union, Geneva, Switzerland, Nov. 2014.
- [14] A. S. Sedra and K. C. Smith, *Microelectronic Circuits*. Oxford: Oxford University Press, seventh edition ed., 2015.
- [15] U. Schwark and D. Redman, “Radio Altimeter Interference Susceptibility Testing Status Update,” in *Agenda Item 3: Radio Altimeter and Wireless Aircraft Intra-Communications (WAIC) Issues*, (Montreal, Canada), International Civil Aviation Organization Frequency Spectrum Management Panel, Jan. 2019.

## APPENDIX A

### FULL RESULTS FOR IN BAND TESTING

The results of all five altimeters presented to the FSMP in [15] are presented here. The results were summarized in Table 3.1. The breaking point was as described in Section 2.6.2, and consists of any reported altitude (i) labeled NCD (ii) with a maximum height error  $\geq \pm 2\%$ , or (iii) any mean height error  $\geq \pm 5\%$ . Interference power thresholds were then set 2 dB below the breaking point of the worst performing altimeter (RA Type 4).

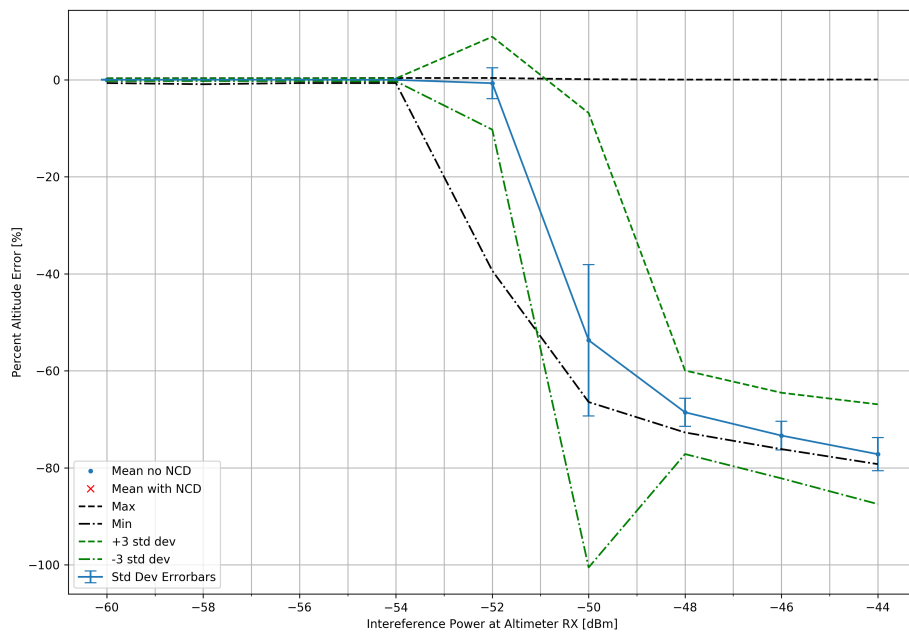


Figure A.1: Performance of RA Type 1 with 200MHz In Band Tests

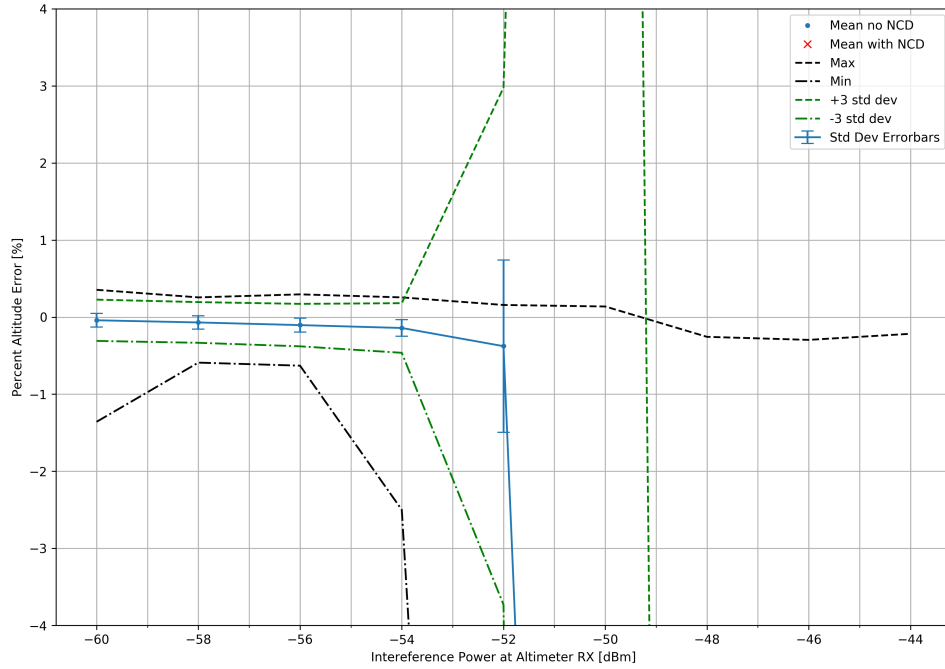


Figure A.2: Performance of RA Type 2 with 200MHz In Band Tests

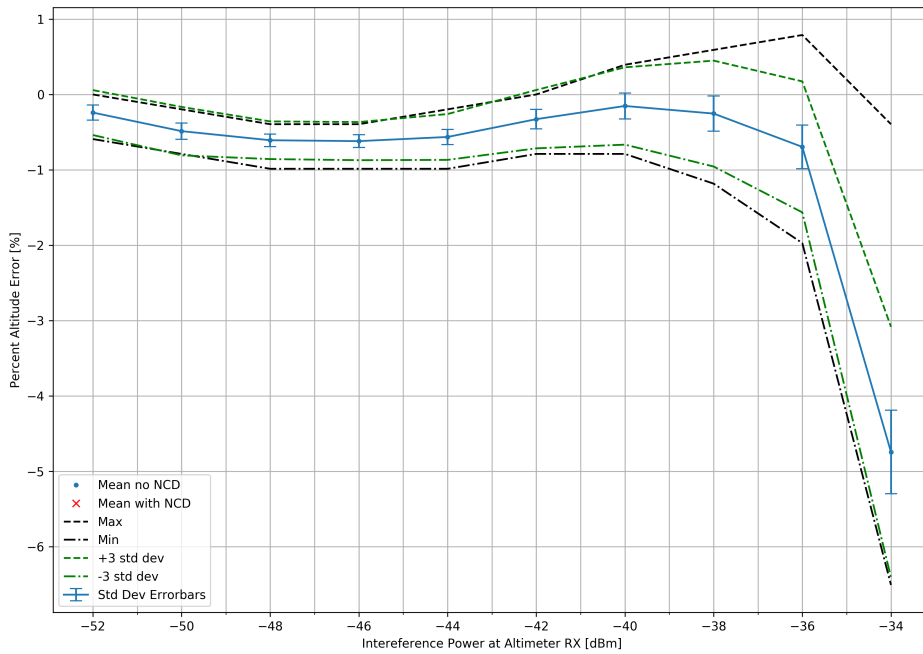


Figure A.3: Performance of RA Type 3 with 200MHz In Band Tests

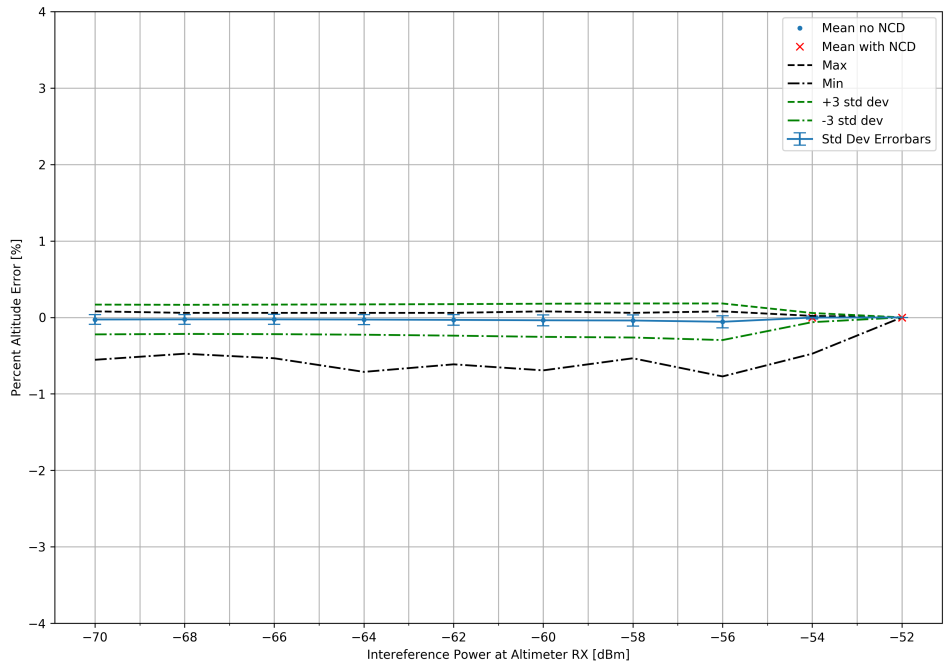


Figure A.4: Performance of RA Type 4 with 200MHz In Band Tests

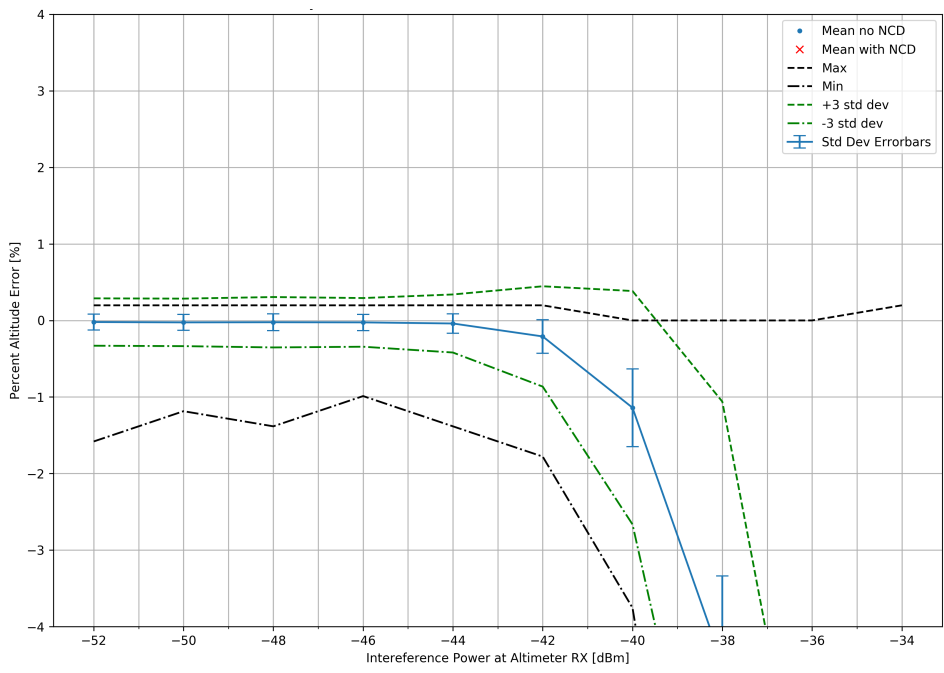


Figure A.5: Performance of RA Type 5 with 200MHz In Band Tests